Master Thesis

Document status: final version

Evaluation of hydrological models under stationary and non-stationary conditions

Da Li

University of Twente

Date: December 1, 2020

Supervisors:

Dr. Ir. M.J. Booij

University of Twente, Faculty of Engineering Technology, Water Management

Dr. M.S. Krol

University of Twente, Faculty of Engineering Technology, Water Management

Acknowledgement

This research is the final work to finish my master student career in the Civil Engineering program at the University of Twente in Enschede. The research title is 'Evaluation of hydrological models under stationary and non-stationary conditions', and from the start to the almost end, I feel increasingly interested in the project and what I am doing on it. The reason I chose this project is from the courses I had before the thesis, the teachers (professors) are so professional in this area, and I am attracted by the knowledge they teach and the method they use. Gradually, I find learning a project which study climate change impact on runoff by hydrological models would be interesting. Fortunately, I found one by having a nice talk with Martijn Booij who is one of my supervisors for my thesis. He talked a lot about hydrological modeling, which make me firmly study this project.

I am so grateful to my two supervisors (Martijn Booij and Maarten Krol), I can finish this research without their professional and patiently guidance. They give me a lot of suggestions in the completement of this research and corrects many mistakes I made and was going to made. We cooperate on this research for more than 11 months (including research proposal), during this period, we had many meetings for discussing periodic learning and during which they give me a lot of suggestions to do series of steps on the research. And during each meeting, we enjoyed it no matter we meet online or face to face. For every document I sent to them, they can give efficient and useful feedbacks, and even not in the meeting they answered my questions in detail by email even in late night, which make my study going in right direction.

I want to thank my family for supporting me to study abroad, they gave me a lot of motivation and courage to finish my master's degree. They are my strong backing.

Finally, I learnt large amount of knowledge about hydrology because of doing this research. I think even in the future, I will continue to work for this area.

Da Li

University of Twente, Enschede, the Netherlands

11/11/2020

Summary

Climate change impacts on river runoff are unavoidable under different periods of climatic conditions. Hydrological models can be used to assess climate change impacts on river runoff in future periods. Research has shown that both non-stationary and stationary hydrological models are widely used to simulate runoff under climate change impact. This study starts from the hypothesis which is that correlations between optimal model parameters and climatic characteristics may exist, and this can be used to estimate parameter values when applying non-stationary models. The goal of this study is to determine correlations between parameters and climatic characteristics, compare the simulation performance of a non-stationary model with regression equations and a stationary model , and assess climate change impact on runoff with both models in future periods.

The *Genie Rural à 4 paramètres Journalier* (GR4J) model is used and applied to the Chikaskia River Near Blackwell in Oklahoma state in the United States. The observed historical climate data, and GCM-RCM projected historical and future climate data in this catchment are used in this study to achieve the study goal. Objective function Kling-Gupta efficiency (KGE) is used to compare simulated runoff with observed runoff. According to the sensitivity analysis, parameter X_1 (mm) has the most influence on overall model output variable, while the other three parameters show a similar influence on the model output. All four parameters are used to determine correlations with climatic characteristics. Pearson correlation analysis shows that parameter X_1 (mm) has significant correlations with 4 climatic characteristics, and X_4 (d) has significant correlations with 9 climatic characteristics. Parameter X_2 (mm/d) and X_3 (mm) have no significant correlations with any climatic characteristic.

Linear regression analysis is used to establish regression equations to estimate time-varying values of X_1 (mm) and X_4 (d) based on significant correlations. Hydrological reasoning is used to develop the relationships between parameters and climatic characteristics. The parameters with no significant correlations with climatic characteristics are recalibrated, and then used as fixed values in following simulations. In simulations with non-stationary model, consecutive 10 years are used as a hydrological 10-year time window in both calibration and validation periods. Therefore, in this study there are 20 hydrological 10-year time windows in the calibration period (excluding the first year as the warm-up year) and 15 hydrological 10-year time windows in the validation period. With the fixed parameter values, the non-stationary parameters with significant correlations with climatic characteristics are re-optimized for each hydrological 10-year time window in the calibration period. In this way, the regression equations are updated, and this is called re-determination of regression equations. Then the validation is done with the

redetermined regression equations for X_1 (mm) and X_4 (d) to test the robustness of the regression equations. To determine whether either the calibration period or the validation period is more suitable to determine regression equations, the reverse order is done using the period 1972-2001 as the calibration period and the period of 1948-1971 as the validation period. In this study, regression equations from the sequential order calibration and validation are selected because the validation result is better. Then with the stationary model and non-stationary model, the runoff is simulated with observed inputs, GCM-RCM simulated historical inputs and two GCM-RCM future inputs, respectively, to compare which model is more suitable for climate change impact assessment.

Validation	Stationary	Non-stationary
KGE value	0.81	0.70

Concluding, in this study case, the stationary model performs better than the non-stationary model when simulating runoff with observed model inputs when compared to observed runoff (see the table above), one problem accounting this might be due to overparameterization of the optimal model parameter values. However, the non-stationary model performs better than the stationary model when simulating runoff with GCM-RCM historical inputs when compared to observed runoff. In this study, two greenhouse gas emission scenarios (GHG) are used to predict future model inputs, GCM-RCM rcp4.5 projection and GCM-RCM rcp8.5 projection, respectively. Within each scenario, two future periods (period of 2045-2065 and period of 2075-2095) are used for climate change impact assessment on runoff. For both models, climate change impact will result in larger decreased runoff with GCM-RCM rcp4.5 inputs than increased runoff with GCM-RCM rcp8.5 inputs during 2045-2065, and result in larger increased runoff with GCM-RCM rcp8.5 inputs than decreased runoff with GCM-RCM rcp4.5 inputs during 2075-2095.

The determination of the relationships between model parameters and climatic characteristics in the non-stationary model can be improved, since the application of the regression equations for future conditions results for example in unrealistically high values of parameter X_4 (d). Therefore, several recommendations are proposed that might assist in determining the potential relationships between optimal parameter values and climatic characteristics and in applying the non-stationary model for assessing climate change impacts on runoff in future research. For example, analyze the hydrological relationships between the parameters and the significant climatic characteristics, then test the regression equations for one specific parameter with different number of the climatic characteristics, after that select one regression equation with best performance to estimate optimal parameters in the following steps.

List of figures

List of tables

Table of Contents

Chapter 1

Introduction

For simulating runoff in catchments, stationary hydrological models are generally used, especially for the past. With increasing recognition of different factors influencing hydrological models, stationary models are not considered as robust enough to simulate catchment runoff. Non-stationary hydrological models are introduced and used to compare simulation performance with stationary models. The sources of non-stationarity acting on hydrological models are from various aspects, this is described in section 1.1. In this study, both stationary and non-stationary hydrological models are going to be used and compared to test which model is more robust and suitable for runoff simulation for both historical and future periods. Merz et al. (2011) indicate that potential correlations between model parameters and climatic characteristics probably exist. Knoben (2013), based on the study of Merz et al. (2011), investigated the relationships between optimum parameters and climate variables, and important correlations between 4 HBV (The Hydrologiska Byrns Vattenbalansavdelning) hydrological model parameters and 5 climatic characteristics were obtained by using regression analysis. For testing the performance of non-stationary model, new correlations between parameters and climatic characteristics in this study catchment are going to be determined and verified. And the climate change impact assessment on river runoff will be evaluated with taking parameter non-stationarity into the hydrological model.

Chapter 1 introduces changing hydrological behavior and parameter non-stationarity, respectively. The problem definition presents a summary of recent research on climate change and describe the importance of integrating parameter non-stationarity into models for modeling hydrological conditions in section 1.1. Research objectives are described after introducing the two aspects which are related to climate change, and research questions are formulated to achieve the research goals in section 1.2. Section 1.3 introduces the reading guidance of the following chapters.

1.1 Problem definition

1.1.1 Changing hydrological behavior

Climate change is inevitable from one time period to another one, global mean temperature (GMT) is one of the impact results. The global mean temperature was assessed to increase by 1.1 ℃ to 2.9 ℃ due to climate change according to the lowest greenhouse gas emission scenario

from 1990 to 2100. While according to the highest greenhouse gas emission scenario, the GMT would increase by 2.4 ℃ to 6.4 ℃ (Smith et al., 2009). Smith et al. (2009) argued that the risks of extreme weather events will increase dramatically, which will cause huge loss and damage of life and property in no matter developing countries or developed countries. In fact, changing hydrological behavior is caused not only due to climate change, but also due to land use (cover) change and anthropogenic interventions. The fifth assessment report of the IPCC (IPCC, 2014) points that human influence contributes a lot to climate change, which is caused by the increases of greenhouse gas (GHG) emissions (Woodward et al., 2014). With climate change in different time periods, river flow regimes could be different. Only using the stationary model sets could have a negative effect on the simulation of the flow regimes under effect of climate change. For example, the model inputs (e.g. precipitation, temperature) could be different under historic and future conditions, therefore the optimal parameter value sets in one model for simulation could be different, which could result in difference in model output when applying stationary and non-stationary models. Xu and Singh (2004) concluded that the hydrological models taking non-stationarity into account usually can simulate more reliable flow conditions under a changing climate.

It is understandable that when applying different hydrological models, different simulated river discharges and trends can be found for different catchments. Some examples can be seen in Table 1.1.

Table 1.1. Some examples of river flow simulation by different models for historic conditions.

Authors	Catchments	Models	Period for calibration and validation	Comparison of calibration and validation results
Merz et al., 2011	273 catchments in Austria	HBV model	Calibration: 1976 – 1981 validation: 1982 - 2006	Q_{95} overestimated: 12%; Q_{50} overestimated: 15%; Q_5 overestimated: 35%.
Booij, 2005	Meuse basin	HBV model (HBV-1, HBV-15 and HBV-118)	Calibration: 1970 – 1984 Validation: 1985 – 1996	Average discharge: small overestimation; Extreme discharge: underestimation.
El-Nasr et al., 2005	Jeker river basin	SWAT model and MIKE SHE model	Calibration: 1986 – 1988 Validation: 1989 - 1991	Average daily flow: underestimation; SWAT model: underestimate the extreme flow and overestimate the minimum flow; MIKE SHE model: slight underestimate the extreme high flow
Tian et al., 2013	Jinhua River basin	GR4J model, HBV model and	Calibration: 1981 - 1990	GR4J model and HBV model: extreme flows increase

		Xinanjiang model	Validation: 1991 – 1995	Xinanjiang model: Extreme flows decrease

From Table 1.1 we can see that the validation results usually show some differences with calibration results. This is due to two reasons: one is that the optimal parameter sets in the calibration period tend to adapt to model structure and data sets used in calibration, while the optimal parameter sets could change when different periods for calibration are used. The other reason is due to the impact of factors like land use change or climate change on the model parameters. In this study, the impact from climate change on models is studied, which is called as model non-stationarity. When considering model non-stationarity, two sources exist: one is model structure, the other one is model parameter. The change of model structure may be caused by changes of catchment characteristics, which is likely related to differences between the growing and non-growing season for plants (Merz et al., 2011). This difference will be influenced by changes of temperature and also lead to a change of evapotranspiration; therefore, it leads to a change in runoff. In this research, the model structure relates to the processes of determining the length of the growing season, this is outside of the model domain.

1.1.2 Parameter non-stationarity

For different calibration periods, optimal parameter sets are different, this is likely caused by climate variables, because in the sub-periods the climatic characteristics may change. Merz et al. (2011) concluded that strong evidence exists to show there are correlations between model parameters and climate variables. Therefore, parameter non-stationarity will be taken into account to assess the impact of climate change on river flows and water resources. The methods to incorporate this non-stationarity into models are related to determination of model parameters (e.g. Coron et al. (2012) determined parameter values in each hydrological 10-year time window), which is that parameters are determined by climatic characteristics with the correlations.

1.1.3 Research gap

Although many studies have been done to predict river flows under future conditions (see, e.g. Booij, 2005; Tian et al., 2013), the accuracy of the predictions still needs to be verified. For the long-term projections, several uncertainties exist no matter from changing climate or land use (cover) change and anthropogenic interventions. Therefore, the stationary model parameter sets which are determined with GCM-RCM projections under future GHG emission scenarios are possible to predict future river flows with certain errors. If the correlations between parameters and climate variables are known, more effective parameters can be set under future conditions.

In Wouter Knoben's study, regression equations between optimal parameters and climatic variables were determined for application in non-stationary model simulation, however, because of the complexity of the problem and the simplicity of the regression method, there could be a big part of inaccuracy in the determination of the correlations. If applying the correlations for simulation under future conditions, the reliability may decrease. In this research therefore, correlations between model parameters and climate variables will be determined for another study area and by using another hydrological model than used by Knoben (2013) to enhance our understanding of non-stationary hydrological model performance. Based on this, climate change impact assessment will be done to determine if a non-stationary model is more appropriate for assessing the impact of climate change compared with a stationary model.

1.2 Research objectives and questions

Research objectives

Based on previous studies and knowledge on hydrological modeling and prediction, the objective of this research is to get correlations between model parameters and climate variables which can be used for predicting hydrological behavior under changing climate and evaluate the impact of climate change on runoff by using a hydrological model which incorporates parameter non-stationarity, and then compare stationary and non-stationary model results. During the process, a stationary model which considers a stationary parameter set and a non-stationary model which considers parameter non-stationarity will be used, their performances will be compared, and then the results will be used for impact assessment of climate change.

Research questions

To achieve the research objective, the following questions are proposed. By answering the questions, the whole work will be guaranteed to process smoothly, and the objective will be completed. The questions are listed as follows:

1. How does the non-stationary model deal with hydrological simulation incorporating parameter non-stationarity compared to the stationary model?
2. Which climatic characteristics are used for determining regression equations for which model parameters?
3. Which model is more robust when comparing validation results for historical simulations?
4. What are the differences in climate change impacts on runoff simulated with the stationary and non-stationary model?

1.3 Research scope and reading guide

The research is intended to increase knowledge about the functioning of hydrological models under changing climate conditions. The selection of the study catchment and hydrological models will be discussed in Chapter 2. The model used will be adapted to cope with changing climate variables and used for climate change impact assessments. Besides, data in the selected catchments will be selected and used for simulation of models. Chapter 3 introduces the methodology which is going to be used throughout the whole thesis, including calibration algorithms and objective functions, the sensitivity of different parameters to runoff, the calibration and validation process as well as the determination of possible correlations between parameters and climatic characteristics, and finally the method to execute climate change impact assessment will be given. Chapter 4 focuses on presenting the results based on the methodology. Chapter 5 will describe the discussion according to the methods and results. The process of chapter 2, 3, 4 and 5 can be found in Figure 1.1. Conclusions will be presented in chapter 6, and future research suggestions and directions will be summarized in short.

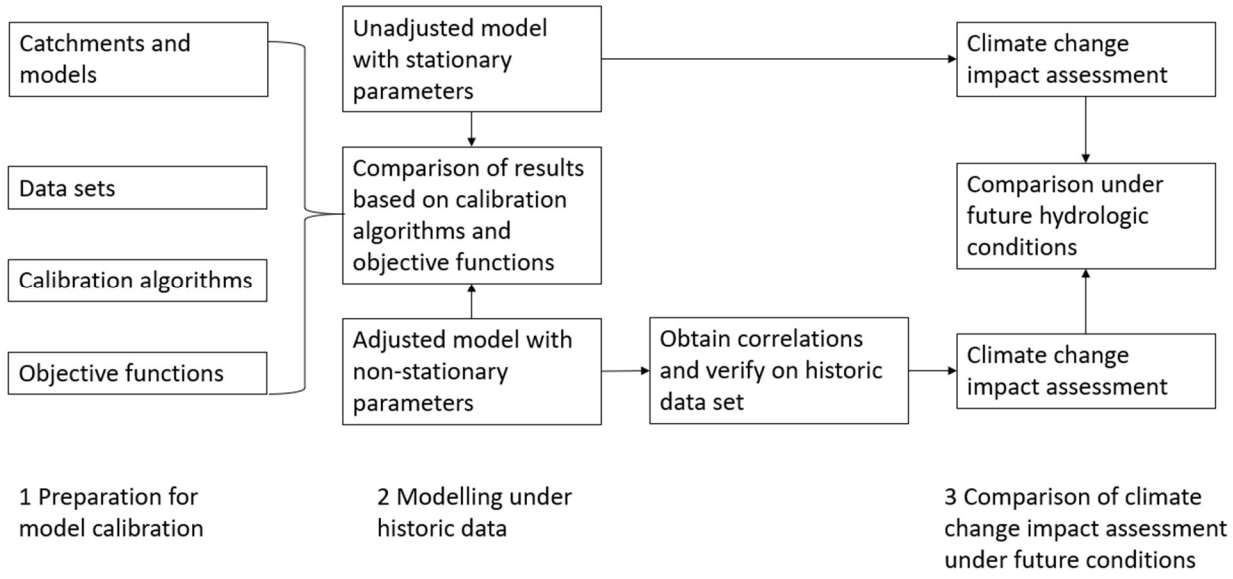

Figure 1.1. Scope of the research.

Chapter 2

Study area and data

This chapter contains information on the selected study area in section 2.1 and collected data in section 2.2. In section 2.3, the model process and parameter functioning will be described in detail.

2.1 Study area

As for this research, GR4J rainfall-runoff model will be applied (discussed in section 2.3), there are no parameters in the model related to snowfall. Therefore, the study area will be selected in a non-snow area or in an area where snowfall only plays a small role in river runoff. Besides, this research is going to focus on the influence of parameter non-stationarity caused by climate change on river discharge, thus, land use change (cover) will try to be avoided in the selected study catchment. The approximate conditions for these two aspects can be found in Figure 2.1. From Figure 2.1, we can see the catchments in the mid-bottom part of the US meet these two requirements in general. In the MOPEX data set (the international Model Parameter Estimation Experiment) for all American catchments, data for 265 catchments are available (https://hydrology.nws.noaa.gov/pub/gcip/mopex/US_Data/), the boundaries of the catchments are shown in Figure 2.2, the small figure is the selected study catchment (discussed in the following part).

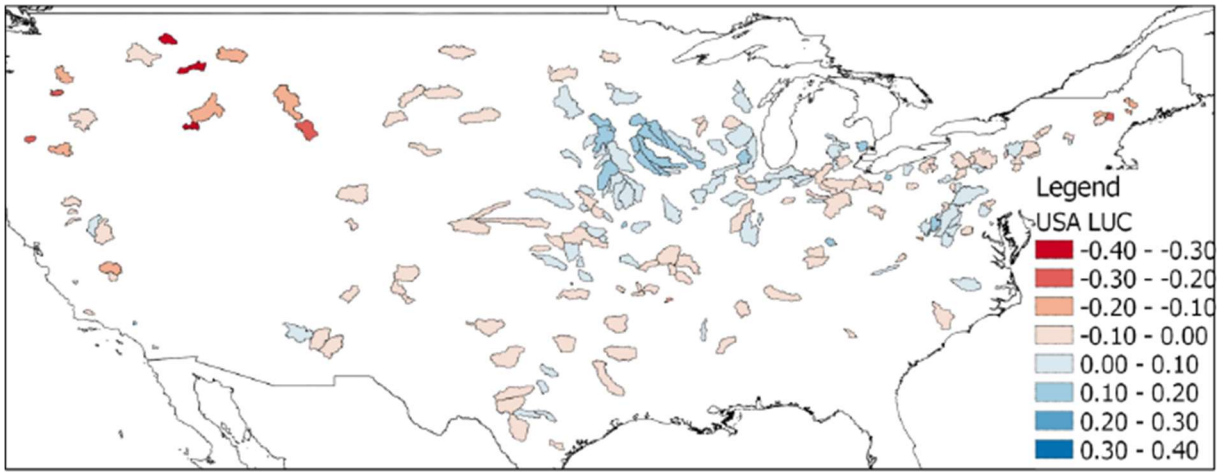

(a)

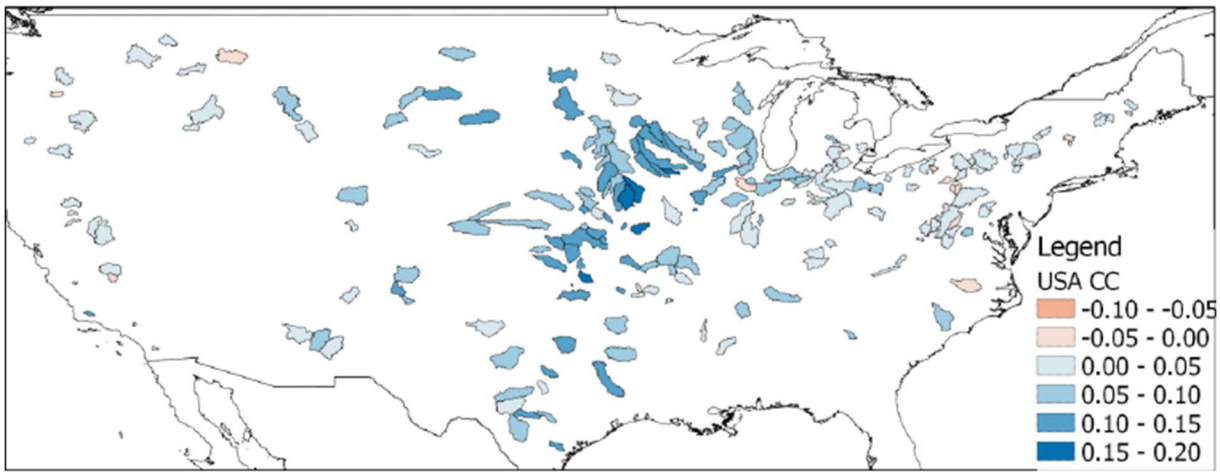

(b)

Figure 2.1 Spatial distribution of changes in streamflow due to land use change (LUC) (a) and climate change (CC) (b) of American catchments, with the historical data of 1950. (Source: Schipper, 2017).

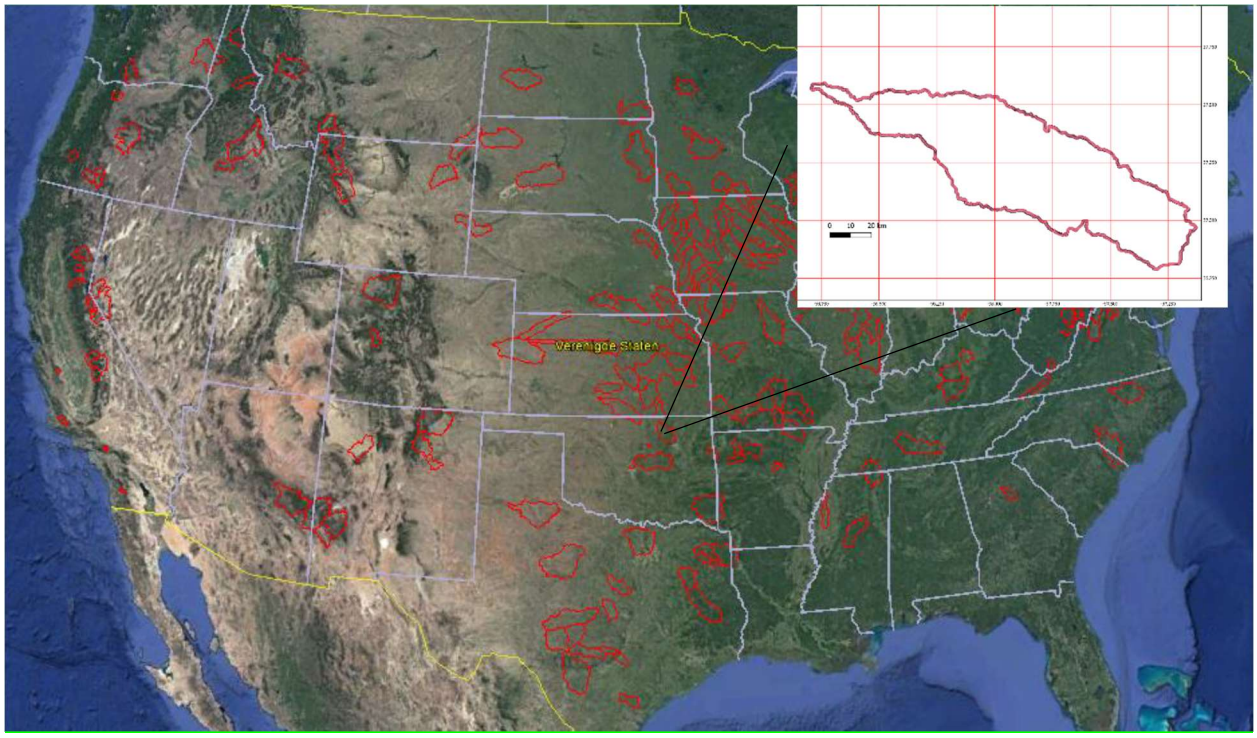

Figure 2.2 Boundaries of 265 catchments in United States (big figure), the boundary in the small figure is the target study area in Oklahoma state. (Source: Schipper, 2017).

The catchment with ID 07152000 is used in this study, which is described as “Chikaskia River Near Blackwell”. The Chikaskia river is a 256-kilometer-long tributary of the Salt Fork of the Arkansas River in southern Kansas and northern Oklahoma in the United States, and it is also a part of the catchment of the Mississippi River. The river in this catchment only contains a small length near

Blackwell city, which has a flow discharge of 17 m^3/s and an elevation of 298 m above mean sea level. The Chikaskia catchment has an area of 4815 km^2, and the climate can be summarized as "Temperate - Without dry season – Hot summer" (Blazs et al., 2003). The average latitude and longitude are 36.8110 and -97.2770 in decimal degrees. According to the University of Maryland (UMD), the most important two vegetation types in this catchment are grassland and cropland with fractional coverage of 0.15 and 0.81, respectively (MOPEX Data). The boundary of this catchment can be found in Figure 2.2.

2.2 Data collection

This section contains two types of data series that will be used in this research, historical observed data and future predicted data. Both data sets at least include data values of precipitation, potential evapotranspiration, and temperature as daily values.

Historical observed data set

This data set can be obtained from the MOPEX dataset, and the daily historical observations of precipitation (P , mm) processed in NWS hydrology Laboratory, climatological potential evapotranspiration (PET_c , mm) based on NOAA Evaporation Atlas, highest and lowest temperature (T, °C) and discharge obtained from USGS National Water Information System can be found during the period of 01-01-1948 to 31-12-2001 for 07152000 catchment in OK. The changing of climate is a process which experience a long-time length, normally considered at least 30 years. The total time length for this catchment is 54 years with complete data values. For making sure the time series is long enough, the data from the whole time series are used.

For the data of potential evapotranspiration, the provided data series cannot be used directly as model inputs because they are climatological potential evapotranspiration. The daily PET values should be calculated with the climatological PET data. The method can be found in Appendix B (Schipper, 2017). P, calculated PET and T are used as model input, runoff data is the output of the model, which are used for calibration and validation of the model.

Historical and future dataset from GCM-RCM projections

The historical dataset from GCM-RCM projections is used to check the accuracy of GCM-RCM predictions by comparing data from GCM-RCM historical projections and data from the observed historical period. The datasets are available from NA-CORDEX which provides detailed data information (Mearns et al., 2017). For example, for the historical data, the description of the variables in the data file can be found in Table 2.1. The future datasets are used to study the

climate change impact on river runoff as model inputs under future conditions. The detailed information of the selected data source can be found in Appendix A.

Table 2.1 Description of variables in each dataset file.

Climatic characteristics	Scenario	GCM	RCM	Frequency	Grid	Bias correction
$Prec$	historical	CanESM2	CanRCM4	Day	NAM-22i	mbcn-Daymet
T_{max}	historical	CanESM2	CanRCM4	Day	NAM-22i	mbcn-Daymet
T_{min}	historical	CanESM2	CanRCM4	Day	NAM-22i	mbcn-Daymet

Bias-correction

As raw data are uncorrected model output, bias-correction needs to be done to the raw data for simulation. In NA-CORDEX, the N-dimensional probability density function transform is adapted for use as a multivariate bias correction algorithm (MBCn) for climate model projections of multiple climate variables (Mearns et al., 2017). MBCn is a multivariate generalization of quantile mapping, which converts all aspects of the observed continuous multivariate distribution into the corresponding multivariate distribution of the variables in the climate model (Cannon, 2018). The datasets have been adjusted using Cannon's MBCn algorithm against a gridded daily observational dataset (Daymet gridded observational datasets) (Mearns et al., 2017). The Daymet dataset interpolates and extrapolates GHCND (Global Historical Climatology Network Daily) station data using statistical methods, and this dataset covers the entire United States.

Calculation of data in study catchment

The future data are estimated with a 0.25-degree spatial resolution. Here a weighted average method is used to calculate data in the whole catchment, which can be expressed as:

$$CC = \frac{P_1 D_1 + P_2 D_2 + \cdots + P_n D_n}{P_1 + P_2 + \cdots + P_n} \quad \text{(2.1)}$$

Where, CC is the climatic characteristic which will be used to estimate future discharge; P_i is the percentage of corresponding catchment area accounting for each lon-lat grid; D_i is the climatic characteristic data in each lon-lat grid, such as P, T_{max} and T_{min}; n is the number of lon-lat grids occupied by the catchment.

With this method, the future data of precipitation, maximum and minimum temperature are available. For calculating potential evapotranspiration for the future period, climatological evapotranspiration values are needed. In observed data, there are 365 PET_c data in each normal year but 366 PET_c data in leap years. However, there are no leap years in future period from the

GCM-RCM rcp projections, thus, the climatological PET data in normal years are used. The method to calculate corrected PET data with T_{max} and T_{min} is the same as described above (in Appendix B).

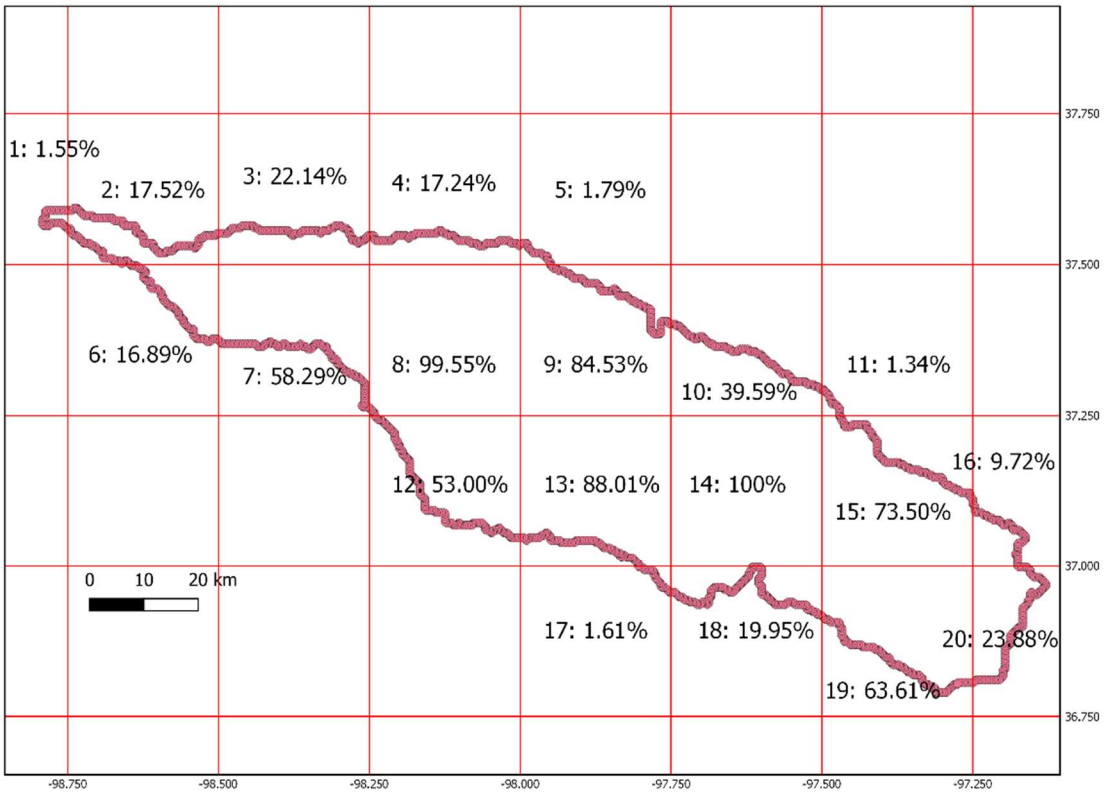

Figure 2.3. Shape of the target catchment 07152000. The number and the percentages indicate the grid cells and the ratio of the corresponding area for each grid cell.

2.3 Description of model

Model choice

For the selection of a hydrological model in this research, firstly the parameters of the model can be affected by climate change, which means it is possible that the parameters could have some relations with different climate conditions. The parameters in the selected model should potentially have the relations. Secondly the model structure can be outside of domain, then the non-stationarity of model parameters can be focused. Thirdly the model can have a relatively accurate reflection when simulating a certain hydrological process, which means the model output has acceptable results compared to observed runoff. Although a variety of models exists, each has its own strengths and drawbacks. No matter physically based models, empirical models,

or conceptual hydrological models, they are all widely used to simulate hydrological processes in different river catchments. However, conceptual models generally can represent the most relevant hydrological processes at the catchment scale (Wheater, 2002), one specification of conceptual models is that the parameters do not necessarily have a physical, but a conceptual interpretation (Pechlivanidis et al., 2011). The correlations between parameters and climatic variables are conceptual but not physical relationship, therefore, in this study a conceptual model is used.

GR4J (*Genie Rural à 4 paramètres Journalier*) rainfall-runoff hydrological model as a conceptual model is used in this study, which was developed by Perrin et al. (2003) based on the GR3J model and was proven being a solid and efficient model in hydrological modeling. GR3J rainfall-runoff model as an empirical model was originally proposed by Edijatno and Michel (1989) and improved by Nascimento (1995) and Edijatno et al. (1999). See the diagram of GR3J and GR4J in Figure 2.4 and parameters in Table 2.2.

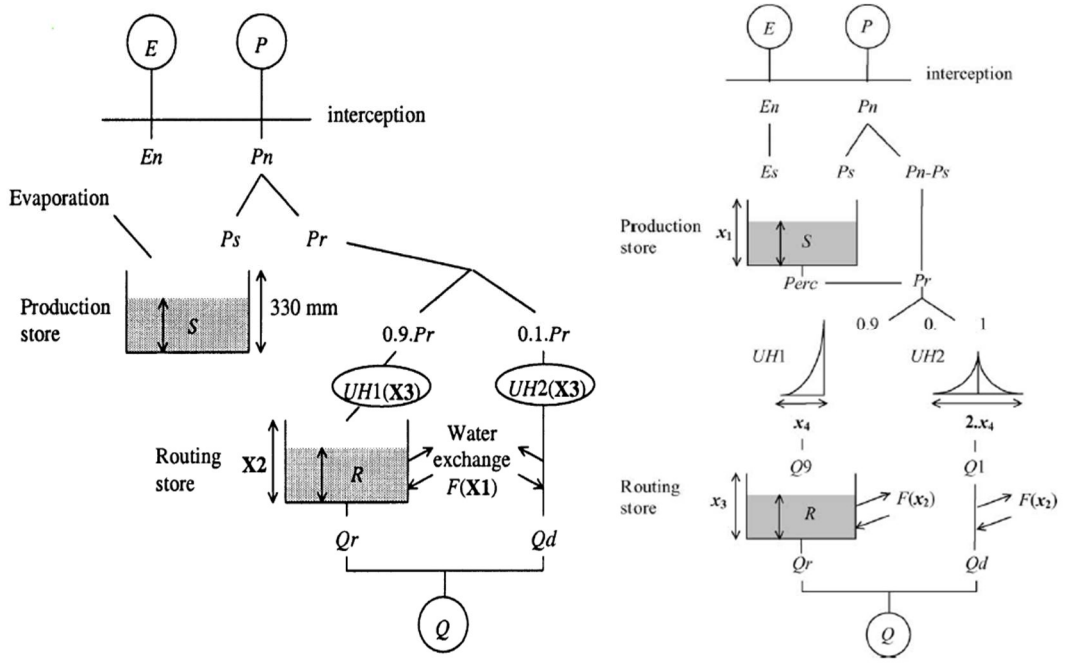

(a) (b)

Figure 2.4 Diagram of GR3J (a) and GR4J (b) rainfall-runoff model (Source: (a) Andreassian et al., 2001 and (b) Perrin et al., 2003).

Table 2.2 List of parameters of the GR3J and GR4J models.

Model	Parameter	Parameter signification
GR3J	X_1	Water exchange coefficient (mm)
	X_2	Capacity of the non-linear routing reservoir (mm)
	X_3	Unit hydrograph time base (day)

GR4J	X_1	Maximum capacity of production store (mm)
	X_2	Groundwater exchange coefficient (mm/d)
	X_3	Maximum capacity of routing store (mm)
	X_4	Time peak ordinate of hydrograph unit *UH1* (day)

Compared with the HBV model (Lindstrom et al., 1997), the GR4J model has a smaller number of parameters, therefore, theoretically less correlations between parameters and climatic characteristics can be addressed, and less equations need to be determined. Totally, GR4J rainfall-runoff model is a suitable model for this study to model the relations between parameters and climatic characteristics.

Model description

In the following, the calculation steps throughout the model are introduced at a given time step. The rainfall depth $P$and the potential evapotranspiration PET are the inputs to the model. The data can be computed by any interpolation method from available rain gauges.

The first step is to compare P and PET and determine either a net evapotranspiration E_n or a net rainfall P_n. In the GR4J model, the interception storage is assumed as zero capacity. P_n and E_n are computed with the following equations:

If $P \geq E$, then:

$$P_n = P - E, E_n = 0 \quad \text{(2.2)}$$

otherwise:

$$E_n = E - P, P_n = 0 \quad \text{(2.3)}$$

In case P_n is not equal to zero, P_s as a part of P_n will fill the production store. It can be calculated with the net rainfall P_n, the actual level S in the production store and the maximum capacity of the store (X_1, mm), the equation is described as:

$$P_s = \frac{x_1\left(1-\left(\frac{S}{x_1}\right)^2\right)\tanh\left(\frac{P_n}{x_1}\right)}{1+\frac{S}{x_1}\tanh\left(\frac{P_n}{x_1}\right)} \quad \text{(2.4)}$$

In the other case, when E_n is not zero, a part E_s of E_n will evaporate from the production store, which can be calculated with the net evapotranspiration capacity E_n, the actual level in production S (mm) and the maximum capacity of the store X_1 (mm). Then the water level is updated by eq. 2.6. The equations are written as:

$$E_s = \frac{S\left(2-\frac{S}{x_1}\right)\tanh\left(\frac{E_n}{x_1}\right)}{1+\left(1-\frac{S}{x_1}\right)\tanh\left(\frac{E_n}{x_1}\right)} \quad \text{(2.5)}$$

$$S = S - E_s + P_s \quad \text{(2.6)}$$

Noted that S is always lower than X_1 (mm). The percolation $Perc$ (eq. 2.7) is taken from the updated water content (eq. 2.6) of the production store and added to the routing part P_r (eq. 2.9). $Perc$ is always lower than S. The level S in the production store is updated as eq. 2.8:

$$Perc = S\left\{1 - \left[1 + (\tfrac{4}{9}\,\tfrac{S}{x_1})^4\right]^{-1/4}\right\} \quad \text{(2.7)}$$

$$S = S - Perc \quad \text{(2.8)}$$

$$P_r = Perc + (P_n - P_s) \quad \text{(2.9)}$$

P_r is divided into two flow components: one part accounts for 90% of P_r and is routed by a unit hydrograph $UH1$ with base time X_4 (d) for delayed runoff; the other part accounts for 10% of P_r and streams into direct runoff by a unit hydrograph $UH2$ with base time $2X_4$. A groundwater exchange term F that acts on both flow components, is then calculated as:

$$F = x_2(\frac{R}{x_3})^{7/2} \quad \text{(2.10)}$$

where R is the level in the routing store, X_3 (mm) is the maximum capacity of the routing store, X_2 (mm/d) is the water exchange coefficient. The value of X_2 (mm/d) can be either positive, negative or zero. A positive value means water imports, while a negative value means water exports, and zero means there is no water exchange. The higher the level in the routing store, the larger the exchange. Note that, F cannot be greater than X_2 (mm/d). In special conditions when the level in the routing store equals X_3 (mm), X_2 (mm/d) represents the maximum quantity of water that can be added (or released) to (from) each model flow component.

The actual level in the routing store is updated using $Q9$ from $UH1$ and F:

$$R = \max(0; R + Q9 + F) \quad \text{(2.11)}$$

The outflow Q_r from the routing store is then calculated as:

$$Q_r = R\left\{1 - \left[1 + \left(\frac{R}{x_3}\right)^4\right]^{-1/4}\right\} \quad \text{(2.12)}$$

Q_r is always lower than R. The level in the reservoir is then reupdated as:

$$R = R - Q_r \quad \text{(2.13)}$$

Noted that the level R can never exceed the capacity X_3 (mm) at the end of a time step.

The output $Q1$ from $UH2$ is expected to have the same water exchange F, then the flow component Q_d is:

$$Q_d = \max(0;\ Q_1 + F) \quad \text{(2.14)}$$

Finally, total streamflow Q is obtained as:

$Q = Q_r + Q_d$ ..... (2.15)

Considering from the MOPEX dataset which provides data of P, PET, T and discharge Q, the inputs of GR4J model are precipitation P and potential evapotranspiration PET, the output is discharge Q.

Parameter range

An initial parameter set for the optimization algorithm calibrating the model parameters is needed. In this research, the initial parameter set, and parameter ranges follow the set from Perrin et al. (2003). Because the values have been obtained on a large variety of catchments (see Table 2.3). If the modeled parameter value is the highest or the lowest value of the parameter range, then the default parameter ranges can be adjusted according to simulated optimal parameters.

Table 2.3. Initial four parameter values and 80% confidence intervals.

	Median value	80% Confidence interval
X_1(mm)	350	100 - 1200
X_2(mm/d)	0	-5 to 3
X_3(mm)	90	20 - 300
X_4(day)	1.7	1.1 - 2.9

Chapter 3

Methodology

This chapter describes methods for answering research questions and reaching the objectives in this study step by step. Section 3.1 describes the sensitivity of the parameters to model output reflected by the objective function. Section 3.2 and section 3.3 introduce the model calibration algorithm and validation arrangement, respectively to describe how non-stationary model incorporates non-stationarity compared with stationary model. In section 3.4, the methods for exploring the correlations and equations between parameters and climatic characteristic are described in detail. In the last section (3.5), the method for climate change impact assessment on river runoff will be introduced, which including the method of how to compare simulation performance of both models to determine which model is more robust under historical period, and the method of climate change impact assessment on rive runoff for both models under future periods.

3.1 Sensitivity analysis

Objective function

An objective function is a widely used statistical method to measure model performance, which is calculated with modeled and observed discharge. The Nash-Sutcliffe coefficient (NSE) (Nash and Sutcliffe, 1970), Mean Square Error (MSE) and Relative Volume Error (RVE) are the three criteria most widely used for calibration and validation of hydrological models. The MSE value can be obtained by dividing MSE by the variance of the observed data and subtracting the ratio from 1. However, in many studies, a combination of different criteria is applied, for example, Xu (1999, NSE and RVE), Bastola et al. (2011, NSE and RVE), Seibert (2003, NSE and groundwater coefficient), Booij et al. (2011, NSE, RVE and Y); Y is calculated by the value of NSE dividing by the sum of 1 plus the absolute value of RVE (Akhtar et al., 2009).

A criterion named Kling-Gupta efficiency (KGE) is proposed, the KGE criterion is proved to be a robust one for describing the statistical relation between simulated discharge and observed discharge (Gupta et al., 2009). Compared to KGE, the MSE criterion is likely to result in an underestimation of the variability in the flows (e.g. a larger underestimation of peak flows). Study examples which use KGE as objective function can be seen from e.g. Knoben et al. (2019), Pool et al. (2018), Franco and Bonuma (2017) and Baez-Villanueva et al. (2018). Totally, in this study, the objective function KGE is used.

The equation of KGE is expressed as:

$$KGE = 1 - \sqrt{(r-1)^2 + (\alpha-1)^2 + (\beta-1)^2} \quad (3.1)$$

where r is the linear correlation between observations and simulations, α is the ratio of the standard deviation of the simulated and observed discharge, and β is a bias term calculated by dividing the average simulated discharge by the average observed discharge:

$$\alpha = \frac{\sigma_{sim}}{\sigma_{obs}} \quad (3.2)$$

$$\beta = \frac{\mu_{sim}}{\mu_{obs}} \quad (3.3)$$

where, σ_{sim} is the standard deviation of the simulated discharge, σ_{obs} is the standard deviation of the observed discharge, μ_{sim} is the average value of simulations and μ_{obs} is the average value of observations. The interval of the value of KGE is $[-\infty, 1]$. Only when the simulations are equal to the observations, the correlation r is 1, α and β equal 1, then the value of KGE equals 1, which means a perfect simulation of the model.

Univariate sensitivity analysis

The sensitivity of $GR4J$ model parameters in the calibration period is investigated. By doing this, the sensitivity of model parameters to model output and sensitivity of model output to model parameters can be analyzed, studying the more sensitive parameters is more meaningful because these parameters affect model output more when climate change impact has obvious influence on the values of the parameters. A univariate sensitivity analysis method is carried out. Firstly, the optimized parameters are calibrated within the calibration period (30 years), which are the values of parameters with 100% percentage. By doing this, we can see the effects of changing parameters around the optimal parameter set. The equations for determining the values of parameters and the relative change are expressed as follows:

$$X_n = X_{optimized} * P_i \quad (3.4)$$

$$X_{scaled} = (X_n - X_{min})/(X_{max} - X_{min}) \quad (3.5)$$

Where, X_n is model parameter, n is a series of value sets for each parameter, $X_{optimized}$ is the optimized parameter values within the calibration period. P_i is used for determining parameter values by multiplying optimized parameters. X_{max} and X_{min} are the maximum and minimum values in X_n, respectively. The relative change values can be used for plotting figures as scaled values, which can make parameter ranges the same.

3.2 Calibration and validation

Before calibration starts, warming up the model is necessary to decrease the influence of initial conditions and make the model reach a normal state. The warm-up period depends on initial conditions of the catchment (e.g. soil wetness) and input data (e.g. rainfall amount). The typical suggested warm-up period ranges from one to several years (Kim et al., 2018). In this study, the total length of data record in the catchment includes 54 years, and for each simulation the simulation period includes at least 10 years, therefore, the first year before each simulation is selected as the warm-up period. In each calibration process, the criteria '*fminsearchbnd*' in Mat-Lab is applied to find the optimal parameter set, and the calibrated optimal parameter set is used in the validation period. During both processes, the observed runoff is needed as the baseline.

3.2.1 Stationary calibration and validation

In the stationary case, all parameters are considered as fixed values. The whole historical period is divided into two parts, calibration period and validation period, respectively. Considering that this study will explore the effect of climate change on parameters, and the parameters will be calibrated within the calibration period, it is better to include at least 30 years when studying climate change impacts. Therefore, the calibration period includes the first 30 years of the total 54 years (1948-1977), and the validation period includes the other part with 24 years (1978-2001).

3.2.2 Method for dealing with parameter non-stationarity

When considering the parameters are affected by climate change, non-stationarity in model parameters need to be considered. The whole response time is divided into multiple time windows of a certain length. For example, Knoben (2013) applied 5-year time windows from a total response time of 30 years in a study of non-stationary hydrological model parameters for the Polish Welna catchment. Coron et al. (2012) used a 10-year sliding window to test combinations of calibration-validation periods in a study of crash testing hydrological models in contrasted climate conditions in Australian catchments. The entire data set in this study is divided into overlapping 10-year time slices, resulting in 20 time slices with different climatic characteristics in the calibration period (11 years when including the warm-up year) and 15 time slices in the validation period. For instance, in the calibration period from 1948-1977, for the first calibration of the first 10-year time slice, 1948 is used as warm-up period, 1949-1958 is used for calibration; for the second calibration of the second 10-year time slice, 1949 is used as warm-up period and 1950-1959 is used for calibration.. The GR4J model is calibrated for each 10-year period to find optimal parameter sets for the climatic conditions during each of the 20 time periods.

3.2.3 Correlations

Climatic characteristics

A goal of this study is to find if there are potential relationships between parameters and specific climatic characteristics to explore the non-stationarity of parameters due to climate change, and then, the climatic characteristics can also be used to determine the parameter values for future conditions. As it is not known that which climatic characteristics are related to optimal model parameters, then multiple climatic variables related to model inputs are used. The applied climatic characteristics can be found in Table 3.1. The climatic characteristics are determined with data in each 10-year time period. All the calculated data are based on daily values.

Table 3.1. Selected climatic characteristics and their meanings.

Climatic characteristics	Meaning
P (mm)	Average precipitation
AET (mm)	Average actual evapotranspiration
PET (mm)	Average potential evapotranspiration
T (°C)	Average temperature
P_{wet} (mm)	Average precipitation intensity on days with P > 0.1 mm
ar	Average aridity
P_{sd} (mm)	Standard deviation of average precipitation
T_{sd} (°C)	Standard deviation of average temperature
P_s (mm)	Average precipitation in summer
T_s(°C)	Average temperature in summer
PET_s (mm)	Average potential evapotranspiration in summer
ar_s	Aridity in summer
$P_{wet,s}$ (mm)	Average precipitation intensity on days with P > 0.1 mm in summer
P_w (mm)	Average precipitation in winter
T_w (°C)	Average temperature in winter
PET_w (mm)	Average potential evapotranspiration in winter
ar_w	Aridity in winter
$P_{wet,w}$ (mm)	Average precipitation intensity on days with P > 0.1 mm in winter

The average temperature T (°C) can be obtained by averaging daily maximum and minimum temperature. The average aridity is the average potential evapotranspiration divided by the average precipitation. Here the climatic variables in summer and winter are selected, because by comparing different seasons, summer and winter can show the changing features of different climatic characteristics, such as P (mm), PET (mm) and T (°C).

Pearson correlation coefficient

The Pearson correlation coefficient (r; Davis, 2002) is used to determine the linear correlations between 20 optimal parameter values and climatic characteristics from 20 10-year time slices. Due to the uncertainty in the relationships between parameters and climate characteristics, this

linear approach is used firstly. The Pearson correlation coefficient can be calculated with covariance between two variables x and y dividing by their standard deviations, which can be expressed as:

$$r = \frac{cov_{x,y}}{\sigma_x \sigma_y} \quad (3.6)$$

r = 1 indicates a perfect positive correlation, while r = -1 indicates a perfect negative correlation. To determine which correlations are statistically significant, the significance level of 5% (p < 0.05) is used as a threshold, which can be tested with Mat-Lab functions '$fitlm$' and '$anova$' (Dumouchel & O'Brien, 1989; Holland & Welsch, 1977; Huber, 1981; Street et al., 1988). Only for correlations with a significance level higher than 0.05, the relevant climatic characteristics will be considered.

3.3 Linear regression analysis

Regression analysis is applied here to establish which climatic characteristics are statistically significant to determine equations for parameter values. First, in this study, single linear regression is used to show the relationship between one independent climatic variable and one dependent parameter. Second, multiple linear regression analysis is executed to determine the relationship between multiple independent climatic variables and one dependent parameter, where the climatic variables used in the multiple linear regression analysis are the significant ones from the results of single linear regression analysis. The Mat-Lab functions '$fitlm$' and '$anova$' can be used in both single and multiple linear regression analysis. The Mat-Lab functions '$fitlm$' creates a linear regression model by fitting to data of dependent parameters and independent climatic variables, and it can also provide the R^2 value which indicates the goodness of fit of the regression line, the higher the R^2 value, the better the regression model. The Mat-Lab function '$anova$' displays a summary analysis of variance table with the p-value for the regression model as a whole. In this study, four model parameters are the dependent variables, and 19 climatic characteristics are the independent variables. All four parameters are tested with single linear regression analysis firstly.

3.3.1 Single linear regression analysis

As it is unlikely to find a perfect relationship between a parameter and all climatic characteristics and therefore the optimal value of a model parameter, single linear regression analysis is applied firstly to screen which climatic characteristic has a statistically significant correlation with a model parameter by adjudging if its p -value is lower than 0.05. For a single linear regression model, its equation can be expressed as:

$$y_r = c_0 + c_1 x_i \quad (3.7)$$

Where, y_r is the dependent parameter and x_i is the independent climatic variable, the constant value c_0 is the linear and pairwise interaction term with y_r , c_1 is the coefficient of the independent climatic variable. In the case of single linear regression, the strength of the regression equation (R^2) is equal to the squared value of the Pearson correlation coefficient r between both variables. This single regression equation also means just one climatic characteristic is used to estimate the optimal parameter value. However, more than one climatic characteristic can affect the parameter, and then it is not robust to estimate the optimal parameter value based on just one climatic characteristic.

3.3.2 Multiple linear regression analysis

Multiple linear regression analysis is used to create a linear regression equation for parameter values by combining multiple significant climatic characteristics. The equation is shown as:

$$y_r = c_0 + c_1x_1 + c_2x_2 + \cdots + c_nx_n \quad \text{.....(3.8)}$$

Where, y_r is the dependent parameter and x_1, x_2,…, x_n are the independent climatic variables which have significant correlations with the parameter, and the constant value c_0 is the linear and pairwise interaction term, c_1 , c_2 ,…, c_n are the coefficients of the independent climatic variable. By combining all significant climatic characteristics into one linear regression analysis does not mean they will contribute a regression equation with highest R^2 value for estimating an optimal parameter value, because they may interact inside the regression model which can make some climatic characteristics non-significant for this linear equation, for instance, an individual climatic characteristic has a statistical significance level lower than 0.05 in the single linear regression, but when using this climatic characteristic in the multiple linear regression model, it is possible that it has a statistical significance level much higher than 0.05. In this case, this climatic characteristic need to be removed from the multiple regression model. The rule to execute this is to remove the climatic characteristic one by one starting with the highest p-value above 0.05 until all the remaining climatic characteristics have a statistical significance level lower than 0.05. Theoretically, with removing the climatic characteristics with a p-value higher than 0.05 one by one, the goodness of fit of the regression equation (R^2) will become higher and higher, this means the regression equation is becoming more robust to estimate optimal parameter values.

3.3.3 Recalibration and revalidation

If all parameters have their own regression equations, the parameters in the validation period will be calculated with the equations. To test the robustness of the regression equations, simulation will be done with optimized parameters by calibrating 20 hydrological blocks in the

calibration period and estimated parameters calculated with regression equations in the validation period.

Recalibration

Another condition which is possible to happen is that some parameters can be calculated with their own regression equations, while for other parameters no significant regression equation is identified. This happens to the parameters for which no significant is found with any climatic characteristic. In this case, these parameters remain stationary but are recalibrated to make them compatible with a variety of calculated values of the parameters which have regression equations. The recalibration period is the same as the stationary case with the first 30 years as calibration period. During the recalibration, the parameters with regression equations are set as temporary 'fixed' values obtained by the regression equations, and the parameters with no regression equations are recalibrated with parameter ranges of the 80% confidence interval.

Redetermination of regression equations

After recalibration, the parameters with no regression equations can be seen as stationary parameters due to no significant correlations between them and climatic characteristics. The reason for redetermining regression equations is that the preliminary equations are determined with optimized four parameters and climatic characteristics in 20 10-year time periods, in which the parameter values are influenced with each other during the optimization process due to the internal interaction of model parameters. The optimized values of parameters which have significant correlations with climatic characteristics may change when applying the stationary parameters. Therefore, the regression equations for the non-stationary parameters are redetermined with new parameters optimized from 20 10-year time periods. After getting the new optimized parameter values, the steps above are repeated to determine new regression equations. By doing this, indeed the parameters for the determination of regression equations are influenced less by fixed parameters. Theoretically, more repeated processes can lead to a more robust determination of equations. However, it is not possible to repeat again and again. The recommendation for this process in further study is given in Chapter 6.

Performance of regression equations in validation period

After the new regression equations are determined for parameters which have significant correlations with climatic characteristics, the non-stationary parameters in the validation period are calculated with the new regression equations. Comparison of the differences between calculated parameters by regression equations with climatic characteristics and optimized parameters in the validation period is done. By doing this, it can test if the regression equations

have good performance in estimating optimal parameter values. If the estimated parameter values with regression equations are close to optimized parameter values, then the regression equations are reliable to be applied in following simulations.

Although the parameters and climatic characteristics are obtained with 10-year time slices, considering about the hydrological year in each time slice, the data in the middle year is actually simulated in each time slice because the estimation of parameters are based on averaged climatic characteristics over 10 years. For instance, the climatic characteristics are calculated from 1949-1958, the parameters calculated by the regression equation stand for the parameters in 1953, therefore, the simulated output stands for the output in 1953.

3.3.4 Reverse order of calibration and validation

The steps above to determine regression equations are using the calibration period and test the performance of simulation using the validation period. With climate change in the whole historical period, however, it may happen that the regression equations obtained with data in the validation period perform better than the regression equations obtained with data in the calibration period. Therefore, the reverse order is done to test the results with 1972-2001 as the calibration period and 1948-1971 as the validation period. The whole process is repeated to determine the regression equations with the new calibration period and test the equations with the new validation period. Therefore, two sets of regression equations are obtained using sequential-order and reverse-order calibration periods. The regression equations resulting in a higher value of the objective function in the validation period will be selected for following simulations.

3.4 Climate change impact assessment

This section describes the change in climatic characteristics for observed datasets and GCM-GCM projected datasets (section 3.5.1). Section 3.5.2 describes the process and methods of climate change impact assessment, and section 3.5.3 describes how to compare the performance between the stationary and non-stationary model under different simulation periods.

3.4.1 Change in climatic characteristics

The observed data and GCM-RCM projections are used as inputs for both the stationary and non-stationary model, the climatic characteristics are expected to be different under different periods, especially when comparing historical and predicted future data. For example, the annual average temperature is expected to increase. By comparing the change of climatic characteristics in historical and future periods, it can give an insight on how climate change influences model inputs.

3.4.2 Climate change impact assessment method

Because the observed historical runoff cannot be compared directly with simulated future runoff, four steps are done to complete climate change impact assessment. First, observed runoff is compared with simulated runoff for both the stationary and non-stationary model with observed P, PET and T data as inputs. This can show the accuracy of both models and difference between both hydrological models. Second, the simulated runoff based on observed P, PET and T data is compared with simulated runoff based on GCM-RCM projections for the same historical period from both the stationary and non-stationary model. This shows the influence of the GCM-RCM combination on predictions for the same hydrological model. Third, the observed runoff is compared with simulated runoff by both models with GCM-GCM historical projections as inputs, and this shows the accuracy and reliability of the selected GCM-RCM combination and the hydrological model. During these three steps, comparisons of the stationary and non-stationary model are made to judge which model is more robust to simulate runoff under future periods. Fourth, the simulated runoff with GCM-RCM projections for historical period as inputs is compared with simulated runoff with GCM-RCM projections for future periods as inputs for both the stationary and non-stationary model. This shows the influence of expected climate change.

3.4.3 Comparison of performance by the stationary and non-stationary model

Flow-duration-curves are used to visualize changes in frequency of simulated flows and to see the process from high flows to low flows from stationary and non-stationary models. Tables based on seasonal and annual changes of flows are made to compare the accuracy of simulations by both models. Although it is impossible to determine which hydrological model is more accurate to simulate future runoff, we can say which model is most probably to be suitable for simulations of future runoff by comparing model performances under historical and future periods.

Chapter 4

Results

This chapter describes the results based on the methodology. Section 4.1 shows the result of sensitivity between model parameter and model output. Section 4.2 shows the calibration and validation results in stationary model case. In section 4.3, the results of Pearson correlations, single and multiple regression analysis indicate which parameters have significant correlations with climatic characteristics, and the regression equations for model parameters with climatic characteristics are determined. After that, the simulation results with regression equations in validation period are compared to see if the regression equations for parameters perform well. Section 4.4 describes the climate change impact on model inputs and runoff under different periods, and then climate change impact assessment to seasonal flows and annual flows is done. The results show which model is more robust in simulating runoff in historical period, and which model is more suitable for future runoff simulation.

4.1 Univariate sensitivity analysis

From the figure, we can see that around the optimized values, it seems that the sensitivity between X_4 and model output is more obvious than the sensitivities between other three parameters and model. However, this does not mean other parameters are not sensitive to model output, which means with impact of climate change, the changes of these parameters can also have an obvious influence on model output.

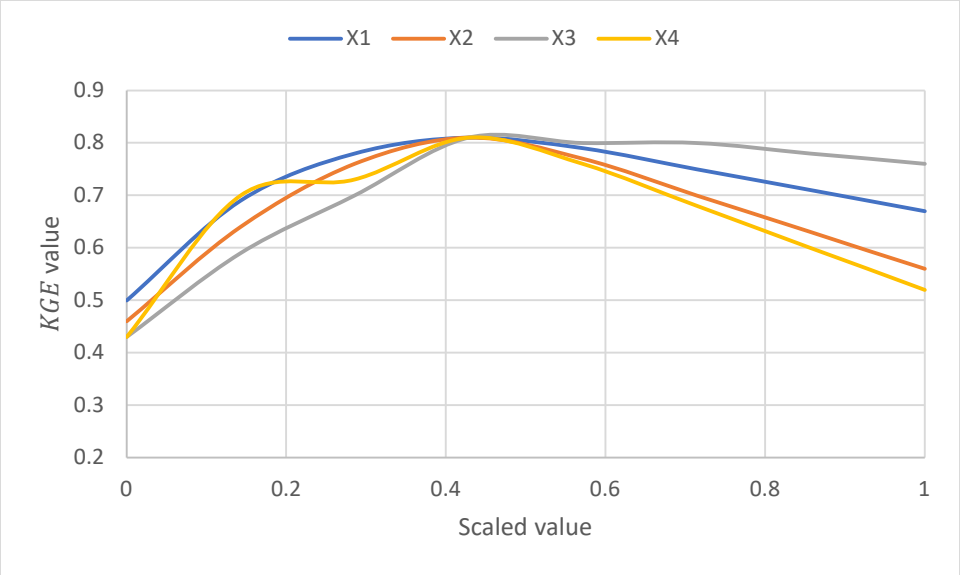

Figure 4.1. Sensitivity between parameters and model output.

4.2 Stationary calibration and validation results

The stationary model used the first 30 years as the calibration period and last 24 years as the validation period. The results show that the parameter value of X_3 (mm) is lower than the default parameter range, to get the optimized parameter value, the lower boundary of the parameter range is lowered to 0.001 mm. The results from sequential and reverse calibration and validation periods are in Table 4.1.

The Kling-Gupta Efficiency (KGE) from calibration in sequential order (0.81) is a little bit worse than the result in reverse order (0.82). The KGE value in the validation period in sequential order (0.79), however, is better than the KGE value in reverse order (0.76). This happens mostly due to the change of input data influenced by climate variability from different periods. It seems that the sequential order is more suitable as a stationary model for comparison with a non-stationary model because of better validation result.

Table 4.1 Stationary calibration and validation results of sequential order and reverse order. In sequential order, the model is calibrated with data from 1948-1977 and validated with data from 1978-2001. In reverse order, the model is calibrated with data from 1972-2001 and validated with data from 1948-1971.

	Sequential		Reverse	
	Calibration	Validation	Calibration	Validation
KGE	0.81	0.79	0.82	0.76

4.3 Correlations for parameters in non-stationary model

4.3.1 Parameters and objective function

The 20 pairs of optimized parameters and their objective function values are plotted in Figure 4.2. Parameter X_2 and X_4 show a similar tendency to some extent, where their values are lowest in the 15th time period, while parameter X_3 shows a opposite tendency, and the value of X_3 reaches the peak value in the 15th time period. Parameter X_1 does not experience an obvious changing process, but it seems that it reaches a lowest value around the 15th period, then increase again. The KGE values generally show a tendency with increasing at first and then decreasing. The KGE value is relatively low in the 15th time window, after that the KGE values increase again to around 0.82. By comparing the climatic inputs between the 15th period and other time periods, we can find that the average precipitation in the 15th time window is relatively low compared to most of the other time windows (4% lower than the average precipitation among all 20 time windows) and hence the aridity is higher than most of other periods. This might be explained by that during arid periods, water is extracted from the ground rather than stored under and on the ground. For a rainfall event, as for the dry ground, the rainfall prefers to fill in the 'empty' soil rather than forms runoff, this could result in a runoff delay. Therefore, a lower X_2 value and X_4 value appear in the relatively driest period. Besides, the average observed discharge in this period is the lowest in all 10-year periods.

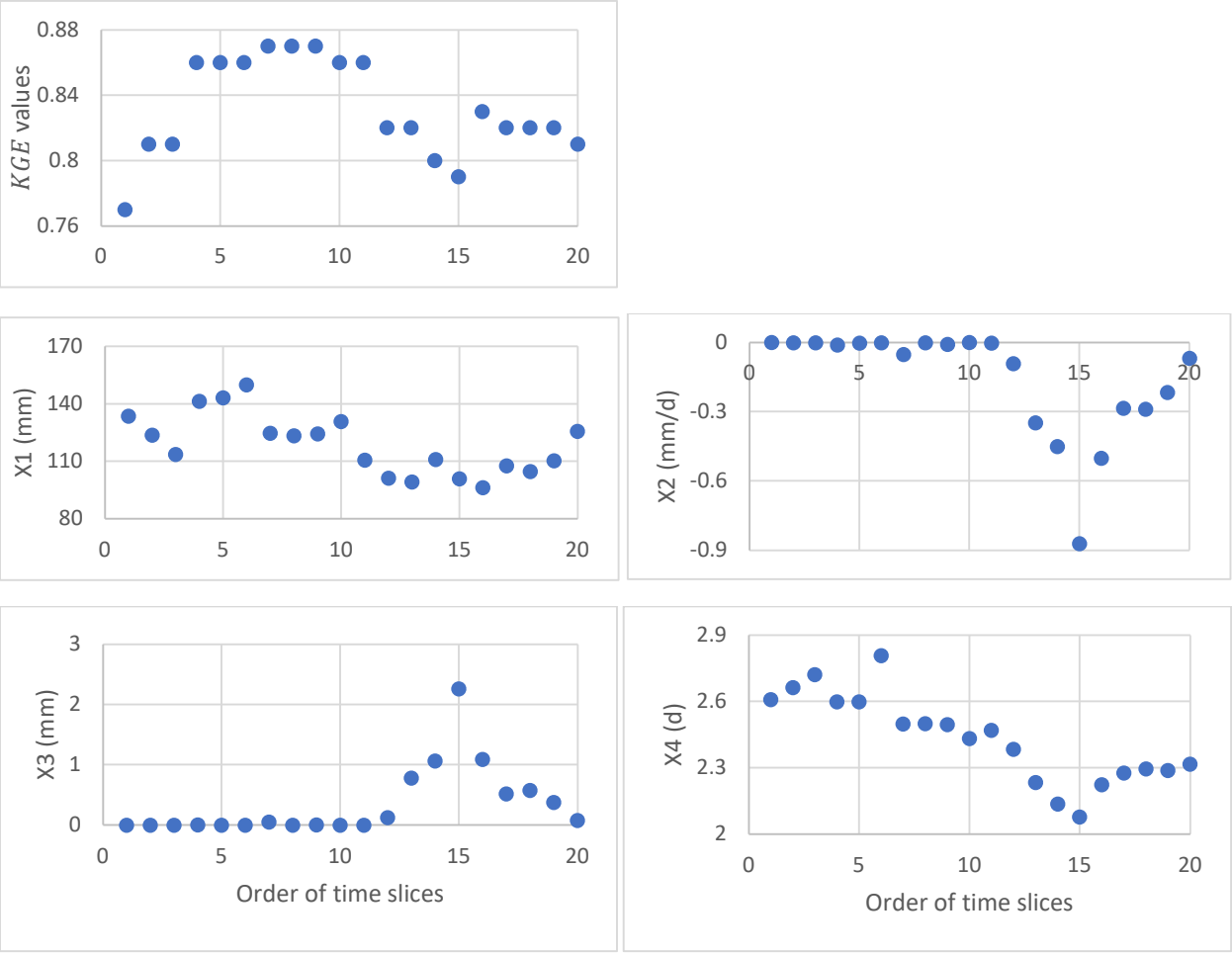

Figure 4.2 Calibration results of 20 10-year time slices. Each time slice includes 10 consecutive hydrological years. The upper figure shows the values of the objective function KGE, the lower four figures show the optimized parameter sets from 20 time slices.

4.3.2 Pearson correlation results

This section gives Pearson correlation results between the four parameters and all climatic characteristics (Table 4.2). Correlations are considered significantly when significance level $p <$ 0.05. The green cells indicate the correlations between parameters and climatic variables are at the 95% level and are discussed, while the white cells indicate the parameters do not show significant correlations with the climatic variables.

Table 4.2. Correlation results between parameters and climatic variables calculated from 20 10-year time windows. Coefficients: r: Pearson correlation coefficients, p: p-value between parameters and climatic characteristics, green: $p < 0.05$ (significant at 95% level), white: $p > 0.05$ (not significant at 95% level).

Climatic variables from 10-year time winows		X1 (mm)		X2 (mm/d)		X3 (mm)		X4(d)	
		r	p	r	p	r	p	r	p
Annual	P (mm)	-0.235	0.318	0.088	0.716	-0.144	0.549	-0.287	0.219
	AET (mm)	-0.393	0.088	-0.177	0.458	0.129	0.591	-0.523	0.018
	PET (mm)	0.479	0.033	0.189	0.425	-0.124	0.601	0.576	0.008
	T (°C)	0.585	0.007	0.349	0.131	-0.276	0.240	0.698	0.001
	Pwet (mm)	0.016	0.944	0.227	0.337	-0.244	0.299	-0.038	0.874
	ar	0.295	0.208	-0.028	0.904	0.087	0.712	0.354	0.127
	Psd (mm)	-0.198	0.401	0.050	0.835	-0.121	0.613	-0.179	0.448
	Tsd (°C)	0.598	0.005	0.386	0.093	-0.309	0.185	0.635	0.003
Summer (JJA)	Ps (mm)	-0.358	0.121	-0.107	0.655	0.121	0.613	-0.329	0.157
	Ts (°C)	0.583	0.007	0.352	0.128	-0.296	0.205	0.710	0.000
	PETs (mm)	0.426	0.060	0.141	0.548	-0.131	0.578	0.427	0.059
	ars	0.384	0.095	0.139	0.559	-0.148	0.534	0.365	0.114
	Pwet,s (mm)	-0.168	0.479	0.032	0.892	-0.016	0.947	-0.199	0.401
Winter (DJF)	Pw (mm)	-0.402	0.079	-0.349	0.132	0.290	0.216	-0.533	0.016
	Tw (°C)	0.297	0.203	0.308	0.187	-0.270	0.249	0.581	0.007
	PETw (mm)	0.330	0.155	0.333	0.153	-0.298	0.205	0.547	0.013
	arw	0.396	0.084	0.358	0.121	-0.307	0.189	0.555	0.011
	Pwet,w (mm)	-0.231	0.328	-0.199	0.402	0.147	0.538	-0.367	0.112

X_1: maximum capacity of production store (mm)

Parameter X_1 (mm) shows all positive correlations with annual PET (mm), T (°C), T_{sd} (°C) and T_s (°C) with significance level higher than 95%.

Parameter X_1 (mm) means the maximum capacity of the production store in the $GR4J$ model, the storage in the production store depends on the replenishment of net PET and net P to the store when the percolation remains the same. If we assume precipitation does not change in a

period, an increased value of X_1 (mm) means the maximum volume for storage increases, then more volume from the difference of P and PET can be stored in the production store, which will lead to less runoff. While increased PET can also lead a decreased directly runoff. Thus, X_1 and PET have a significant positive correlation. When temperature T increases, the soil normally will become drier and the underground water is less, which can lead to an increase of rainfall storage under the ground, therefore increasing T can result in less runoff. Therefore, parameter X_1 and T can have a significant positive correlation. The standard deviation of daily average temperature T_{sd} (°C) can be a monitor of this parameter, when T_{sd} (°C) increases, then parameter X_1 (mm) probably will also increase. The daily average temperature in summer has a significant positive correlation with X_1 (mm), while there is no significant correlation between the daily average temperature in winter and X_1 (mm). This happens probably due to the sensitivity of X_1 (mm) to temperature, the higher the temperature, the more sensitive X_1 (mm) responses to temperature.

X_4: unit hydrograph time base (day)

Parameter X_4 (d) indicates the base time for delayed runoff. Table 4.2 shows there are 9 significant correlations between X_4 (d) and the climatic characteristics. If we take increasing PET as an independent event, then the increased PET (mm) will lead to decreased runoff which can be divided into direct and delayed runoff. When the precipitation does not change, then the direct runoff does not change. While with the increased PET (mm), less water will store in the production store and the routing store firstly, and it also increases the maximum storage of the production store, then lead to runoff, which is called delayed runoff. Therefore, the time for this runoff is delayed more. Increased T (°C) will result in a drier soil moisture, then the rainfall will fill in the drier soil but not a direct runoff, thus result in a delayed runoff. Therefore, daily temperature T (°C) has a strong positive correlation with X_4 (d). It is very strange that the AET (mm) has a strong negative relationship with T (°C), it is expected that AET (mm) has a positive correlation with temperature T (°C), and therefore has a positive correlation with X_4 (d). This might happen that this model is oversensitive to AET (mm), the optimal X_4 (d) might increase to dampen this effect. Results show that the standard deviation of temperature T_{sd} (°C) might be an indicator to see that change of X_4 (d), when T_{sd} (°C) increases, the value of X_4 (d) increases. Both average temperature in summer (T_s, °C) and average temperature in winter (T_w, °C) have a significant correlation with parameter X_4 (d), this could happen if X_4 (d) is not sensitive to high and low temperature. In contrast, parameter X_4 (d) shows obvious sensitivities to the low magnitude of precipitation and potential evapotranspiration. The magnitude of precipitation and potential evapotranspiration in winter is much lower than in summer, and the correlations between P_w (mm) and PET_w (mm) and X_4 (d) (negative and positive, respectively) are significant at 95% level. In summer with much higher P (mm) and PET (mm), the stores maybe saturated at some point, the effect of increased X_4 (d) is thus diminished. While with lower P (mm) and PET (mm) in winter, the decreased P (mm) and increased PET (mm) can increase the aridity, then could have obvious effect on extension of base time for the delayed runoff.

4.3.3 Single and multiple linear regression analysis

This section firstly discusses the single linear regression relationships between model parameters (X_1, mm; and X_4, d) and each climatic characteristic that is at a 95% significance level. Then based on the results from single linear regression analysis, multiple linear regression analysis is done to see if there are regression equations using multiple climate characteristics.

Single linear regression

The single linear regression is done with 20 optimized parameter values and 20 values of climatic characteristics from the 20 10-year time windows. The results show the regression strength R^2 of the correlation between one parameter and one climatic characteristic in Table 4.3. Every single climatic characteristic with 95% significance level can form an independent linear regression equation. The higher the R^2 value, the better the performance of the single regression equation. In Table 4.3, parameter X_1 (mm) has four independent single linear regression equations?, with a regression strength varying from R^2 = 0.19 (with PET, mm) to R^2 = 0.32 (with T_{sd} , °C). The rank of the regression strengths means that when using only one climatic characteristic to estimate the value of X_1 (mm), then T_{sd} (°C) can give the best estimation, while PET (mm) can give the worst estimation. For parameter X_4 (d), there are 9 independent single linear correlations between climatic characteristics and X_4 (d), with regression strengths varying from R^2 = 0.23 (with AET, mm) to R^2 = 0.48 (with T_s, °C), respectively. When only using one climatic characteristic to estimate X_4 (d), the temperature in summer T_s (°C) can give the best estimation and actual evapotranspiration AET (mm) can give the worst estimation among all significant climatic characteristics.

Table 4.3. The regression strength R^2 of single linear regression equations? between model parameters and significant climatic characteristics.

R^2	Significant climatic characteristics								
Parameter	AET(mm)	PET(mm)	T (°C)	Tsd (°C)	Ts (°C)	Pw (mm)	Tw (°C)	PETw (mm)	arw
X1(mm)	-	0.19	0.31	0.32	0.30	-	-	-	-
X4(d)	0.23	0.3	0.46	0.37	0.48	0.24	0.3	0.26	0.27

Multiple linear regression

Parameter estimation with only one climatic characteristic usually cannot give the most accurate results but might do with multiple significant climatic characteristics. All significant climatic variables are included in the regression equation, but due to the interaction of the climatic variables, some climatic variables will show a higher p-value than 0.05 and are not at the 95% significance level anymore. In this case, these climatic variables will be removed one by one until

all remaining climatic variables show p-values lower than 0.05 so that the regression strength increases to the highest value. The regression equation obtained by doing this is seen as the best for parameter estimation. The regression results by removing climatic variables individually is shown in Appendix C.

The regression equations are expressed as:

$$X_1 = C_{1,0} + C_{1,1} * T_{sd} \quad (4.1)$$

$$X_4 = C_{4,1} * PET + C_{4,2} * T + C_{4,3} * T_s \quad (4.2)$$

Where, X_1 (mm) and X_4 (d) are the model parameters and C_n are coefficients of climatic variables. The values of the coefficients are shown in Table 4.4.

Table 4.4 Coefficients in the regression equations for X_1 and X_4.

Coefficients	$C_{1,0}$ (mm)	$C_{1,1}$ (mm/°C)	$C_{4,1}$ (d/mm)	$C_{4,2}$ (d/°C)	$C_{4,3}$ (d/°C)
Values	-768.40	83.74	-8.39	1.34	0.57

4.3.4 Recalibration and revalidation

Results show that parameters X_2 (mm/d) and X_3 (mm) have no significant correlations with all climatic characteristics and they should be considered as fixed values. Therefore, they are recalibrated, while during recalibration, X_1 (mm) and X_4 (d) are constant which are calculated by the regression equations obtained above, and X_1 (mm) and X_4 (d) become non-stationary after recalibration. The recalibration period is the same as in the stationary case, which is 1948-1977 as the recalibration period and 1978-2001 as the revalidation period. The recalibration results are shown in Table 4.5. The objective function KGE values are 0.81 for recalibration and 0.76 for revalidation, respectively.

Table 4.5 Recalibration values of X_2 (mm/d) and X_3 (mm), and calculated values of X_1 (mm) and X_4 (d) during recalibration.

Parameters	X_1 (mm)	X_2 (mm/d)	X_3 (mm)	X_4 (d)
Values	115.2876	-0.0283	0.0247	2.4064

4.3.5 Redetermination of regression equations

As parameters X_2 (mm/d) and X_3 (mm) are fixed values, the influence of interaction between parameters due to different values of X_2 (mm/d) and X_3 (mm) in different calibration periods disappears. The optimal parameter values of X_1 (mm) and X_4 (d) in each 10-year time window should be updated with the fixed X_2 (mm/d) and X_3 (mm). According to the new optimized X_1

(mm) and X_4 (d), the new regression equations can be obtained by repeating the steps described above. The new equations are:

$$X_1 = C_{1,0} + C_{1,1} * ar_w \quad (4.3)$$

$$X_4 = C_{4,1} * PET + C_{4,2} * T + C_{4,3} * PET_w \quad (4.4)$$

The values of the coefficients are shown in Table 4.6.

Table 4.6 Coefficients of climatic variables in new regression equations.

New coefficients	$C_{1,0}$ (mm)	$C_{1,1}$ (mm)	$C_{4,1}$ (d/mm)	$C_{4,2}$ (d/°C)	$C_{4,3}$ (d/mm)
Values	203.24	-46.10	-6.37	1.67	2.43

With the new regression equations, values of parameter X_1 (mm) and X_4 (d) in the validation period can be calculated. Appendix D gives the detailed comparison of optimized parameters and calculated parameters in the validation period to show the robustness of the regression equations. With the new optimized parameters of X_1 (mm) and X_4 (d) in the calibration period and calculated parameter values of X_1 (mm) and X_4 (d) in the validation period, as well as the fixed X_2 (mm/d) and X_3 (mm), simulation for the whole period is done. The objective function KGE is 0.80 for calibration and 0.66 for validation, respectively. The overall results are shown in Table 4.7.

Table 4.7 The objective function KGE results for calibration and validation in different cases under sequential order and reverse order. Stationary case is to calibrate four parameters with the whole calibration period and validate with the whole validation period, non-stationary case is that the parameters X_1 (mm) and X_4 (d) are optimized with fixed X_2 (mm/d) and X_3 (mm) in the calibration period, the parameters X_1 (mm) and X_4 (d) are calculated with the regression equations in the validation period.

	Sequential order		Reverse order	
Cases	calibration	Validation	Calibration	Validation
Stationary	0.81	0.79	0.82	0.76
Non-stationary	0.80	0.66	0.81	0.64

4.3.6 Reverse order of calibration and validation

The whole process including section 4.1 and section 4.2 described above to determine the regression equations is to use 1948-1977 as the calibration period and 1978-2001 as the validation period. The reverse order needs to be done to judge which order is more suitable for obtaining regression equations for parameters for future conditions. Under reverse order, the period of 1972-2001 is used as the calibration period and the period of 1948-1971 is used as the validation period, respectively. The whole process is repeated to determine the regression equations for model parameters. The results are shown in Table 4.7. In the calibration period, the objective function values of KGE under reverse order are better than KGE values under the

sequential order. The validation results under the reverse order, however, are worse than the sequential order. For GCM-RCM historical projection, the selected period for simulation should be as closely as possible to the observed historical validation period. Therefore, the validation results are considered to be more important than the calibration results. Thus, the regression equations obtained under the sequential order should be used in simulations for GCM-RCM historical and future projections.

4.4 Climate change impact assessment

This section describes the results of the climate change impact assessment using the stationary model and non-stationary model with regression equations. For each case, simulation is done by both models to compare the difference between their modeling performances. Section 4.4.1 shows the climatic change impact on model inputs by comparing historical observations and GCM-RCM projected historical inputs and comparing GCM-RCM projected historical and future inputs, respectively. Section 4.4.2 shows the climate change impact assessment on runoff by four comparisons. Table 4.8 describes the case names and their descriptions used in the following analysis, we can find there are 6 30-year periods for simulation including observed historical period, GCM-RCM simulated historical period and GCM-RCM projected future periods. However, in each 30-year period, there are 21 10-year time windows which stand for 21 hydrological years. The data shown in the tables from section 4.4.1 to section 4.4.2 are daily data, μ: the average value; σ: the standard deviation of the daily average per year in each 21-year hydrological period. The units of μ and σ are the same as the units of the variables. The values in green cells means they are overestimated compared to the baselines (the baseline values are used for comparison for other results, e.g. in Table 4.9 (a), the bias (%) is calculated with (3.86 mm-2.85 mm)/2.85mm), while the values in red cells mean they are underestimated compared to the baselines.

Table 4.8 Case names and their descriptions.

Case name	Description of each case
Observed	Observations
Simulated-s	Simulated variables with observations as inputs by stationary model
Simulated-ns	Simulated variables with observations as inputs by non-stationary model
GCM-RCM hist-s	Simulated variables with GCM-RCM historical inputs by stationary model
GCM-RCM hist-ns	Simulated variables with GCM-RCM historical inputs by non-stationary model
Rcp4.5-2041-2070-s	Simulated variables with GCM-RCM rcp4.5 inputs by stationary model for period 2041-2070
Rcp4.5-2041-2070-ns	Simulated variables with GCM-RCM rcp4.5 inputs by non-stationary model for period 2041-2070
Rcp4.5-2071-2100-s	Simulated variables with GCM-RCM rcp4.5 inputs by stationary model for period 2071-2100
Rcp4.5-2071-2100-ns	Simulated variables with GCM-RCM rcp4.5 inputs by non-stationary model for period 2071-2100
Rcp8.5-2041-2070-s	Simulated variables with GCM-RCM rcp8.5 inputs by stationary model for period 2041-2070
Rcp8.5-2041-2070-ns	Simulated variables with GCM-RCM rcp8.5 inputs by non-stationary model for period 2041-2070
Rcp8.5-2071-2100-s	Simulated variables with GCM-RCM rcp8.5 inputs by stationary model for period 2071-2100
Rcp8.5-2071-2100-ns	Simulated variables with GCM-RCM rcp8.5 inputs by non-stationary model for period 2071-2100

4.4.1 Climate change impact on inputs

This section shows the climate change impact on climatic characteristics P (mm), PET (mm) and T (°C) by comparing observed inputs and GCM-RCM projected historical inputs and comparing GCM-RCM projected historical inputs and GCM-RCM projected future inputs, respectively (Table 4.9 and Table 4.10). The climatic inputs are determined as annual average values and seasonal average values for spring (March, April, May; MAM), summer (June, July, August; JJA), autumn (September, October, November; SON) and winter (December, January, February; DJF).

Observed and GCM-RCM historical inputs

In Table 4.9 (a), compared with observed climatic inputs, the GCM-RCM historical projection overestimates average spring and winter precipitation by about 35% and 86%, respectively. While it slightly underestimates average precipitation in summer and autumn by 2% and 2%, respectively. Totally, the annual average precipitation is overestimated with approximately 19% by the GCM-RCM historical projection compared with observed annual precipitation. In Table 4.9 (b), the results show that PET (mm) is overestimated in spring but overestimated in other seasons by GCM-RCM projected historical data compared to the baseline. The annual average PET (mm) is slightly underestimated by the GCM-RCM historical projection. In each season and on an annual scale, the overestimations and underestimations are relatively small. In Table 4.9 (c), GCM-RCM projected historical average temperature in spring and winter is overestimated by 4.76 °C and 1.94 °C respectively, but underestimated in summer and autumn by 1.44 °C and 6.67 °C respectively compared to observed average temperature. The total annual average temperature is slightly underestimated in the same period, only with 0.34 °C.

Totally, the GCM-RCM historical projection overestimates the annual precipitation but underestimates the annual potential evapotranspiration and average temperature compared with observed inputs in the same historical period from 1976-1996.

Table 4.9 Bias of seasonal and annual climatic characteristics P (mm), PET (mm) and T (°C) between observed data and GCM-RCM projected historical data. Three sub-tables are made for: (a) average precipitation, mm; (b) average potential evapotranspiration, mm; and (c) average temperature, °C.

(a)

Precipitation P (mm)	MAM		JJA		SON		DJF		Annual	
Baseline	μ	σ	μ	σ	μ	σ	μ	σ	μ	σ
Observed	2.85	0.78	2.86	1.04	1.94	0.82	0.82	0.49	2.12	0.35
	μ	σ	μ	σ	μ	σ	μ	σ	μ	σ
GCMRCM-hist	3.86	1.07	2.80	1.37	1.90	0.94	1.53	0.90	2.53	0.40
Bias(%)	35.45	37.45	-2.15	31.54	-1.74	14.71	86.11	83.42	19.10	16.29

(b)

PET (mm)	MAM		JJA		SON		DJF		Annual	
Baseline	μ	σ	μ	σ	μ	σ	μ	σ	μ	σ
Observed	4.15	0.27	6.49	0.36	3.34	0.20	1.09	0.16	3.78	0.12
	μ	σ	μ	σ	μ	σ	μ	σ	μ	σ
GCMRCM-hist	4.17	0.15	6.38	0.52	3.33	0.22	1.06	0.09	3.75	0.19
Bias(%)	0.37	-43.10	-1.74	47.33	-0.38	14.42	-2.55	-44.09	-0.87	56.97

(c)

Temperature T (°C)	MAM		JJA		SON		DJF		Annual	
Baseline	μ	σ	μ	σ	μ	σ	μ	σ	μ	σ
Observed	13.87	1.38	26.52	1.04	15.01	0.96	1.68	1.97	14.33	0.66
	μ	σ	μ	σ	μ	σ	μ	σ	μ	σ
GCMRCM-hist	18.63	0.97	25.08	1.88	8.34	1.01	3.62	1.34	13.99	0.82
Bias(°C)	4.76	-0.40	-1.44	0.84	-6.67	0.05	1.94	-0.64	-0.34	0.16

GCM-RCM projected historical and future data

In Table 4.10 (a), for the first period of future projections for both scenarios, precipitation increases in spring but decreases in summer and autumn compared to the precipitation from the GCM-RCM historical projection. Although the precipitation from GCM-RCM rcp4.5 for 2040-2070 decreases but from GCM-RCM rcp8.5 for 2040-2070 increases, the total annual precipitation will increase for both projections. While for the second period of future projections, precipitation from both projections decreases in spring and autumn but increases in summer and winter compared to seasonal precipitation from the GCM-RCM historical projection, and the total annual precipitation will increase for both future scenarios. A trend which can be found in both future scenarios is that the annual precipitation is increasing. And for both periods, GCM-RCM rcp8.5 projection gives higher estimation than GCM-RCM rcp4.5 projection. In Table 4.10 (b), no matter for the first period or for the second period in both scenarios, the changes in seasonal and annual PET (mm) are small, and both projections give increasing annual PET (mm) compared to the projected PET (mm) compared to the GCM-RCM historical projection. A trend in both scenarios seems that the estimation of PET (mm) is increasing from the first period to the second period. In Table 4.10 (c), the average temperature in each future case will increase compared to the average temperature from the GCM-RCM historical projection. From the first period to the second period for both scenarios, the average temperature increases. The GCM-RCM rcp8.5 projection gives a higher estimation than the GCM-RCM rcp4.5 projection in both periods.

Totally, compared to the GCM-RCM historical projection, GCM-GCM rcp4.5 and rcp8.5 projections give decreased precipitation from 2045-2065 but increased precipitation from 2075-2095, and increased potential evapotranspiration and average temperature for both periods. Notably, the GCM-RCM rcp8.5 projection gives higher estimation for precipitation and average temperature than the GCM-RCM rcp4.5 projection for both periods.

Table 4.10 Differences of seasonal and annual climatic characteristics P (mm), PET (mm) and T (°C) between GCM-RCM projected historical data and GCM-RCM projected future data. The GCM-RCM projected historical data are the

baselines. Three sub-tables are made for: (a) average precipitation, mm; (b) average potential evapotranspiration, mm; and (c) average temperature, °C.

(a)

Precipitation P (mm)	MAM		JJA		SON		DJF		Annual	
Baseline	μ	σ	μ	σ	μ	σ	μ	σ	μ	σ
GCM-RCM hist	3.86	1.07	2.80	1.37	1.90	0.94	1.53	0.90	2.53	0.40
	μ	σ	μ	σ	μ	σ	μ	σ	μ	σ
rcp4.5-2041-2070	3.96	0.87	2.54	1.17	1.38	0.53	1.39	0.46	2.32	0.37
Difference(%)	2.46	-18.83	-9.23	-14.11	-27.70	-44.00	-9.21	-49.15	-8.19	-7.48
rcp8.5-2041-2070	4.04	1.09	2.49	0.91	1.82	1.10	1.69	0.70	2.52	0.42
Difference(%)	4.75	2.41	-11.05	-33.41	-4.63	16.69	10.51	-21.68	-0.56	4.13
rcp4.5-2071-2100	3.83	1.18	3.08	0.97	1.48	0.71	1.75	0.66	2.54	0.48
Difference(%)	-0.67	10.27	10.02	-28.86	-22.45	-25.18	15.02	-26.30	0.56	17.86
rcp8.5-2071-2100	3.77	1.13	3.69	1.32	1.71	0.81	2.02	0.81	2.80	0.51
Difference(%)	-2.47	6.13	31.58	-3.76	-10.05	-13.84	32.33	-9.24	10.78	26.42

(b)

PET (mm)	MAM		JJA		SON		DJF		Annual	
Baseline	μ	σ	μ	σ	μ	σ	μ	σ	μ	σ
GCM-RCM hist	4.17	0.15	6.38	0.52	3.33	0.22	1.06	0.09	3.75	0.19
	μ	σ	μ	σ	μ	σ	μ	σ	μ	σ
rcp4.5-2041-2070	4.16	0.22	6.54	0.40	3.38	0.15	1.09	0.11	3.81	0.16
Difference(%)	-0.07	41.88	2.52	-23.40	1.39	-30.97	2.78	26.66	1.57	-13.50
rcp8.5-2041-2070	4.13	0.20	6.49	0.37	3.32	0.22	1.06	0.09	3.77	0.15
Difference(%)	-0.86	31.34	1.82	-28.44	-0.47	-1.22	0.01	4.40	0.44	-20.11
rcp4.5-2071-2100	4.25	0.16	6.52	0.42	3.41	0.17	1.10	0.07	3.84	0.15
Difference(%)	2.10	5.15	2.22	-19.86	2.45	-22.19	3.45	-23.28	2.32	-19.42
rcp8.5-2071-2100	4.23	0.17	6.54	0.38	3.47	0.25	1.10	0.10	3.85	0.17
Difference(%)	1.44	10.61	2.48	-28.05	4.26	9.87	3.23	14.62	2.64	-10.00

(c)

T (°C)	MAM		JJA		SON		DJF		Annual	
Baseline	μ	σ	μ	σ	μ	σ	μ	σ	μ	σ
GCM-RCM hist	18.63	0.97	25.08	1.88	8.34	1.01	3.62	1.34	13.99	0.82
	μ	σ	μ	σ	μ	σ	μ	σ	μ	σ
rcp4.5-2041-2070	21.19	0.90	28.80	1.62	12.11	0.90	6.28	1.49	17.17	0.82
Difference(°C)	2.56	-0.07	3.71	-0.26	3.77	-0.11	2.66	0.15	3.18	0.00
rcp8.5-2041-2070	21.94	1.18	29.95	1.48	12.64	1.20	6.28	1.28	17.78	0.87
Difference(°C)	3.31	0.21	4.87	-0.40	4.30	0.19	2.65	-0.06	3.79	0.05
rcp4.5-2071-2100	21.78	1.02	29.07	1.74	12.81	1.03	6.60	1.05	17.64	0.74
Difference(°C)	3.15	0.05	3.99	-0.15	4.47	0.03	2.98	-0.29	3.65	-0.08
rcp8.5-2071-2100	27.89	1.05	28.48	1.48	9.31	1.40	11.58	1.63	19.39	0.98
Difference(°C)	9.26	0.07	3.40	-0.40	0.96	0.39	7.96	0.29	5.39	0.17

4.4.2 Climate change impact assessment

This section gives the results of the climate change impact assessment with stationary and nonstationary models. First, simulated runoff based on observed climatic inputs is compared with observed runoff to determine model accuracy. Next, simulated runoff based on observed climatic inputs is compared with simulated runoff based on the GCM-RCM historical projection to

determine GCM-RCM influence. After that, the observed runoff is compared with simulated runoff based on GCM-RCM historical projection to determine to influence of the combination of GCM-RCM and hydrological models. Last, simulated runoff based on the GCM-RCM historical projection is compared with simulated runoff based on the GCM-RCM future projections to assess the climate change impacts on runoff. Runoff data are determined for seasonal and annual statistics. Similarly, considering hydrological years in each 30-year period, tables and flow-duration curves are made for the historical period during 1976-1996, the first future period during 2045-2065 and the second period during 2075-2095, respectively.

Influence of hydrological models

Table 4.11 shows the comparison results of the seasonal and annual statistics of observed runoff and simulated runoff based on observed inputs by stationary and nonstationary models. Compared to the observed runoff, simulated runoff with observed P (mm), PET (mm) and T (°C) as inputs is underestimated by both stationary and nonstationary models in both spring and summer, but overestimated in autumn. Although the stationary model gives an overestimated winter runoff and the nonstationary model gives an underestimated winter runoff, the total annual runoff is underestimated by both the stationary model (with 6%) and nonstationary model (17%). The stationary model simulates runoff closer to the observed runoff. The high standard deviation in winter flow by stationary model means daily runoff is less smoothy than observed winter daily runoff, and the much lower standard deviation in winter flow by nonstationary means daily runoff is much more smoothy than observed winter daily runoff. In other seasons, the standard deviation picks similar trend. From the view of annual flow, the annual daily runoff simulated by the nonstationary model is much more smoothy than the annual daily runoff simulated by the stationary model compared to the observed annual daily runoff.

Table 4.11 Seasonal and annual bias between observed discharge and simulated discharge with observed climatic inputs by stationary and nonstationary models. The calculated observed data are the baselines.

Q (mm)	MAM		JJA		SON		DJF		Annual	
Baseline	μ	σ	μ	σ	μ	σ	μ	σ	μ	σ
Observed	0.51	0.45	0.31	0.28	0.28	0.34	0.17	0.13	0.32	0.18
	μ	σ	μ	σ	μ	σ	μ	σ	μ	σ
Simulated-s	0.45	0.33	0.24	0.27	0.33	0.33	0.17	0.13	0.30	0.11
Bias(%)	-11.91	-26.15	-22.92	-5.64	16.68	-5.41	3.64	3.97	-6.33	-39.69
Simulated-ns	0.41	0.32	0.22	0.26	0.31	0.31	0.11	0.10	0.26	0.10
Bias(%)	-18.53	-29.80	-27.74	-9.01	9.35	-9.60	-36.81	-24.54	-17.06	-45.15

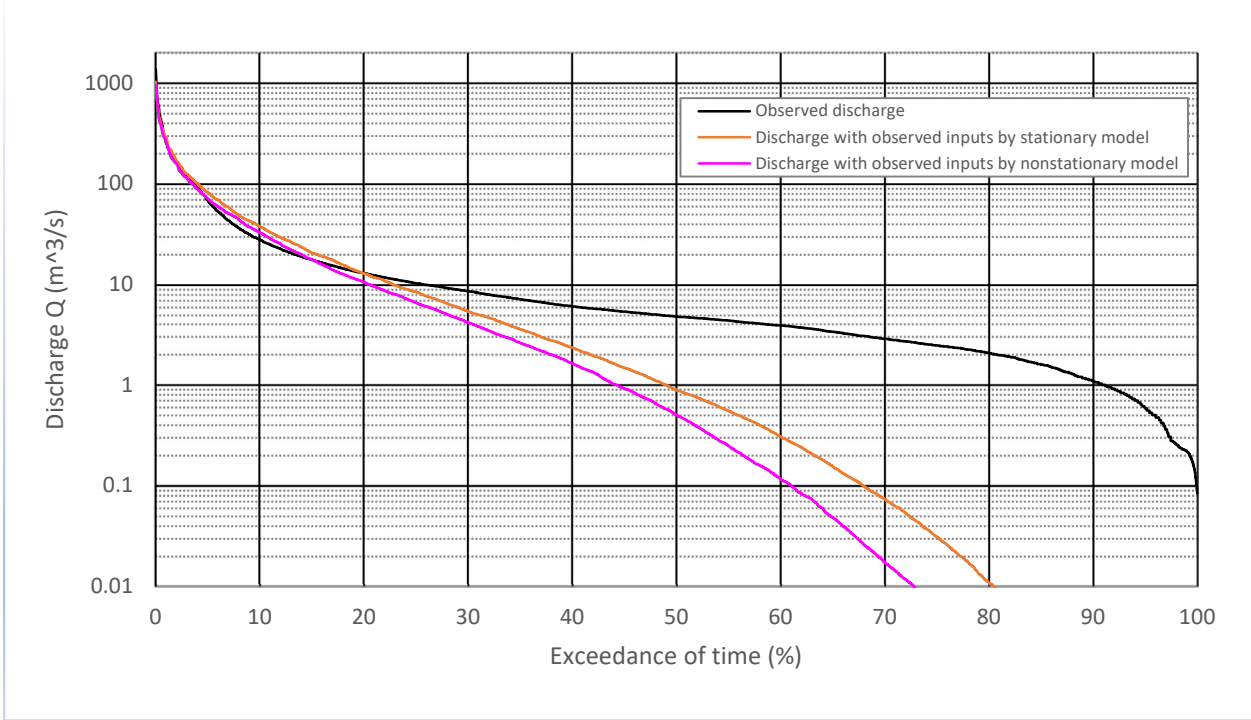

Figure 4.3 Flow duration curves of observed discharge and simulated discharge by both stationary model and nonstationary model with observed inputs for period 1976-1996.

Figure 4.3 shows the flow-duration curves of observed discharge and simulated discharge with observed inputs by both models. For the high flows, the simulated discharges by both stationary and nonstationary models up to an exceedance frequency of around 20% are quite close to observed discharges. Both models underestimate discharges with a higher exceedance frequency than 20% compared to observed discharges. The stationary model, however, simulates low discharges closer to observed low discharges than the nonstationary model.

Totally, the stationary model and the nonstationary model do not give perfect simulations to observed runoff. The objection function values for this period is 0.81 for the stationary model and 0.70 for the nonstationary model, respectively. The stationary model performs better than the nonstationary model when comparing the influence of hydrological models.

Influence of GCM-RCM projection

Table 4.12 shows the comparison of the seasonal and annual discharges between simulated discharge based on observed data and simulated discharge based on GCM-RCM projected historical data for both stationary and nonstationary models. The simulated discharges with GCM-RCM projections as input are much larger than the simulated discharges with observed data when using the stationary model for all seasonal flows and this results in a larger estimation of approximately 83% of the annual discharge. The simulated discharges based on GCM-RCM projected historical data are much larger in spring, summer and winter flows but slightly larger

in autumn flow, and totally the annual discharge is much larger with about 78% compared to simulated discharges based on observed data when using the nonstationary model. Hence the estimations by both models for spring, summer, winter and annual flows are similar when using GCM-RCM historical projection as model inputs compared to using observed data as model inputs. Besides, simulated annual discharge by the nonstationary model results in a lower estimation than the stationary model. For both models, the standard deviations in four seasonal and annual daily runoff are much higher than the baselines, which mean the simulated daily runoff with GCM-RCM historical inputs by both the stationary and nonstationary model are much less smoothy than the simulated daily runoff with observed inputs. The high estimations of standard deviation in the two cases show that the annual daily runoff change from GCM-RCM historical projection has much less stability than the annual daily runoff change simulated based on observed inputs.

Table 4.12 Seasonal and annual discharge difference between simulated discharge based on observations and simulated discharge based on GCM-RCM historical projection for both stationary and nonstationary models. The simulated discharges based on observations by both stationary and nonstationary models are the baselines.

Discharge Q (mm)	MAM		JJA		SON		DJF		Annual	
Baseline	μ	σ	μ	σ	μ	σ	μ	σ	μ	σ
Simulated-s	0.45	0.33	0.24	0.27	0.33	0.33	0.17	0.13	0.30	0.11
GCMRCM-hist-s	0.93	0.45	0.45	0.47	0.33	0.36	0.46	0.35	0.54	0.19
Difference(%)	106.51	34.34	88.76	75.57	1.62	8.99	164.76	165.79	82.60	74.02
Baseline	μ	σ	μ	σ	μ	σ	μ	σ	μ	σ
Simulated-ns	0.41	0.32	0.22	0.26	0.31	0.31	0.11	0.10	0.26	0.10
GCMRCM-hist-ns	0.87	0.44	0.41	0.44	0.30	0.34	0.29	0.31	0.47	0.18
Difference(%)	110.52	37.90	82.59	71.56	-3.10	9.10	174.98	230.46	78.04	81.46

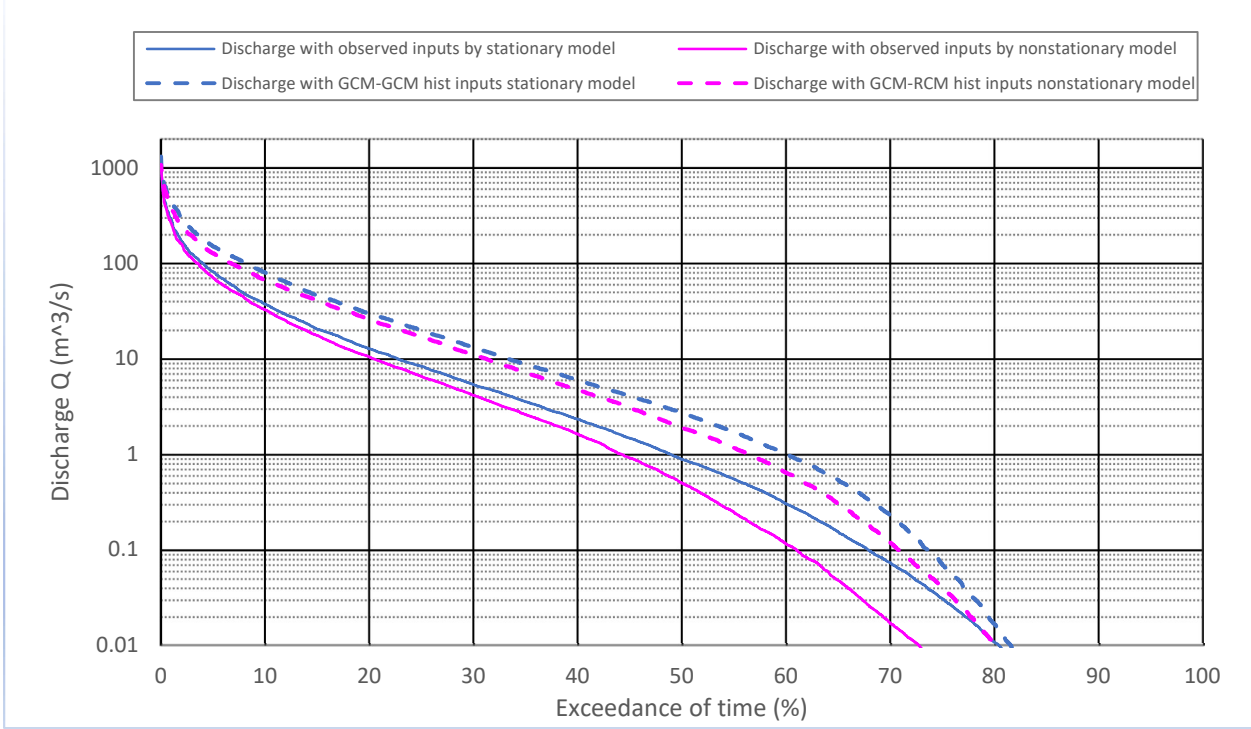

Figure 4.4 Flow duration curves of simulated discharge by stationary and nonstationary model with observed inputs and GCM-RCM historical inputs for period 1976-1996.

Figure 4.4 shows the flow-duration curves of simulated discharge with observed data as inputs and with GCM-RCM historical projection as inputs by both models. A general trend we can find from this figure is that simulated discharges based on observed inputs have a closer change tendency from high flows to low flows with the change of exceedance frequency, while the simulated discharges based on GCM-RCM historical inputs have a closer change tendency from high to low flows with the change of exceedance frequency. When comparing the performance of the two models with the same input source, observed data inputs or GCM-RCM historical inputs, simulated discharges of the nonstationary model are lower than simulated discharges of the stationary model.

In conclusion, from Table 4.12 and Figure 4.4, the simulated discharges based on GCM-RCM historical inputs are much larger than simulated discharges based on observed inputs for both models. The GCM-RCM historical projection seems unsatisfactory to execute runoff simulation. For the future projections, the same GCM-RCM combination is used, thus the simulated discharges based on GCM-RCM future inputs are not that robust.

Influence of combination of GCM-RCM projection and hydrological model

Table 4.13 shows that the GCM-RCM historical projection gives overestimations of discharges in all seasons and for annual flows compared to the observed flows for both models. The simulated discharges with the stationary model show a larger overestimation than simulated discharges with the nonstationary model for all seasonal and annual flows. The nonstationary model with GCM-RCM historical inputs performs better than the stationary model with GCM-RCM historical inputs. The standard deviation shows that the simulated annual discharge change from nonstationary model is more smoothy than the simulated annual discharge from stationary model, this might be resulted by which the standard deviations of daily runoff in all four seasons by the nonstationary are smaller than the standard deviations of daily runoff by the stationary model.

Table 4.13 Bias of seasonal and annual discharges between simulated discharges with stationary and nonstationary model based on GCM-RCM historical projection and observed discharges. The observed discharges are the baseline.

Discharge Q (mm)	MAM		JJA		SON		DJF		Annual	
Baseline	μ	σ	μ	σ	μ	σ	μ	σ	μ	σ
Observed	0.51	0.45	0.31	0.28	0.28	0.34	0.17	0.13	0.32	0.18
	μ	σ	μ	σ	μ	σ	μ	σ	μ	σ
GCMRCM-hist-s	0.93	0.45	0.45	0.47	0.33	0.36	0.46	0.35	0.54	0.19
Bias(%)	81.92	-0.79	45.50	65.66	18.57	3.10	174.38	176.36	71.05	4.94
GCMRCM-hist-ns	0.87	0.44	0.41	0.44	0.30	0.34	0.29	0.31	0.47	0.18
Bias(%)	71.50	-3.20	31.93	56.10	5.96	-1.37	73.76	149.36	47.66	-0.47

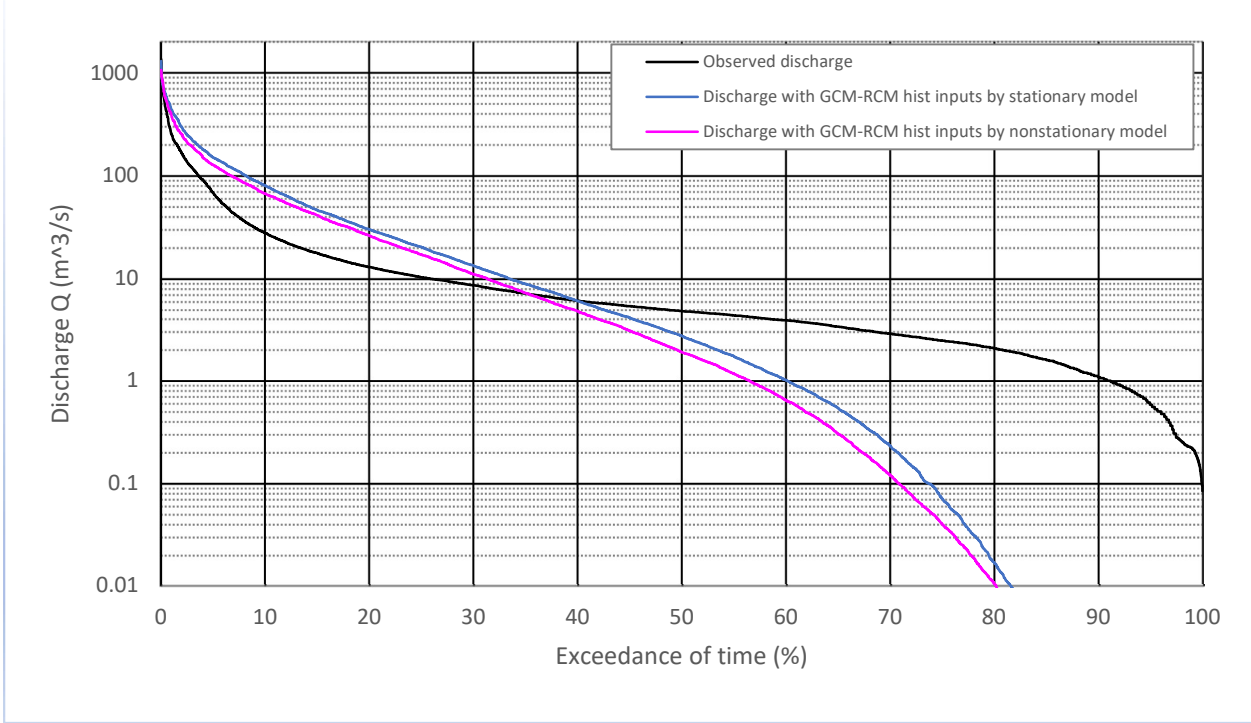

Figure 4.5 Flow duration curves of observed discharge and simulated discharge by both stationary model and nonstationary model with GCM-RCM historical inputs for period 1976-1996.

Figure 4.5 shows the flow duration curves of observed discharge and simulated discharge based on GCM-RCM historical projection with both stationary and nonstationary models. The flow duration curves of simulated discharges by both models show large differences compared to the flow duration curve of observed discharges. The simulated discharges by the stationary model up to an exceedance frequency of 40% are higher than observed discharges and are lower than observed discharges above an exceedance frequency of 40%. While the simulated discharges by the nonstationary model up to an exceedance frequency of about 35% are higher than observed discharges, and above an exceedance frequency of 35% are lower than observed discharges. This figure seems to suggest a balanced over- and underestimation of discharge with GCM-RCM driven inputs compared to observed discharge. However, the average observed daily discharge is about 18 m^3/s, while the average simulated daily discharges by the stationary and nonstationary model are approximately 30 m^3/s and 26 m^3/s, respectively.

Totally, both models with GCM-RCM historical projection as inputs simulate much higher annual runoff than observed runoff. The nonstationary model with an annual runoff overestimation of 48%, however, performs better than the stationary model with an annual overestimation of 71% compared to observed annual runoff when comparing the influence of a combination of GCM-RCM projection and the hydrological model.

Climate change in GCM-RCM historical and future projections

The period of 2045-2065

In Table 4.14, for the simulations with the stationary model, the simulated discharges based on the GCM-RCM rcp4.5 projection show increases in summer, autumn and winter flows but a decrease in spring flow, which result in an increase in annual flows compared to the simulated discharges based on GCM-RCM historical projection. While the simulated discharges based on the GCM-RCM rcp8.5 projection show increases in spring, autumn and winter flows but a decrease in summer flows, which result in an increase in annual flows as well compared to the baseline. According to the absolute value of the annual discharge changes, the GCM-RCM rcp8.5 projection projects a smaller annual discharge change than the GCM-RCM rcp4.5 projection compared to GCM-RCM historical projection. For simulations with the nonstationary model, the simulated discharges based on the GCM-RCM rcp4.5 projection increase in summer, autumn and winter but decrease in spring, from which a decrease with 19% in annual flow is shown when comparing to simulated discharges based on GCM-RCM historical projection. While the simulated discharges based on the GCM-RCM rcp8.5 projection decrease in summer and winter but increase in spring and autumn, and an increase with about 6% in annual flow is shown when comparing to simulated discharges based on GMC-RCM historical projection.

For simulation with stationary and nonstationary model, the simulated annual runoff increases based on the GCM-RCM rcp8.5 projection but decreases based on GCM-RCM rcp4.5 projection. When using the same input source (GCM-RCM rcp4.5 or rcp8.5 projection), the nonstationary model gives a lower annual change than the stationary model.

Table 4.14 Seasonal and annual difference of simulated discharges with GCM-RCM historical projection as inputs and simulated discharges with GCM-RCM rcp4.5 and rcp8.5 projections as inputs for the period of 2045-2065 with stationary and nonstationary model. The baselines are simulated discharges based on GCM-RCM historical inputs by stationary and nonstationary model, respectively.

Q (mm)	MAM		JJA		SON		DJF		Annual	
Baseline	μ	σ	μ	σ	μ	σ	μ	σ	μ	σ
GCM-RCM hist-s	0.93	0.45	0.45	0.47	0.33	0.36	0.46	0.35	0.54	0.19
	μ	σ	μ	σ	μ	σ	μ	σ	μ	σ
rcp4.5-2041-2070-s	0.96	0.45	0.28	0.32	0.15	0.17	0.39	0.27	0.44	0.17
Difference(%)	3.21	1.26	-38.82	-31.23	-53.89	-52.80	-15.64	-22.45	-18.24	-14.33
rcp8.5-2041-2070-s	1.16	0.51	0.28	0.32	0.39	0.53	0.50	0.33	0.58	0.17
Difference(%)	25.44	13.18	-38.98	-31.55	17.14	49.19	8.30	-4.05	7.08	-12.13
Baseline	μ	σ	μ	σ	μ	σ	μ	σ	μ	σ
GCM-RCM hist-ns	0.87	0.44	0.41	0.44	0.30	0.34	0.29	0.31	0.47	0.18
	μ	σ	μ	σ	μ	σ	μ	σ	μ	σ
rcp4.5-2041-2070-ns	0.88	0.43	0.28	0.32	0.10	0.14	0.25	0.24	0.38	0.16
Difference(%)	1.11	-0.40	-32.58	-26.84	-65.38	-59.13	-13.42	-22.74	-19.02	-15.28
rcp8.5-2041-2070-ns	1.13	0.48	0.25	0.29	0.33	0.47	0.27	0.29	0.50	0.16
Difference(%)	29.77	10.29	-38.35	-35.64	11.39	39.00	-5.55	-8.85	6.45	-11.78

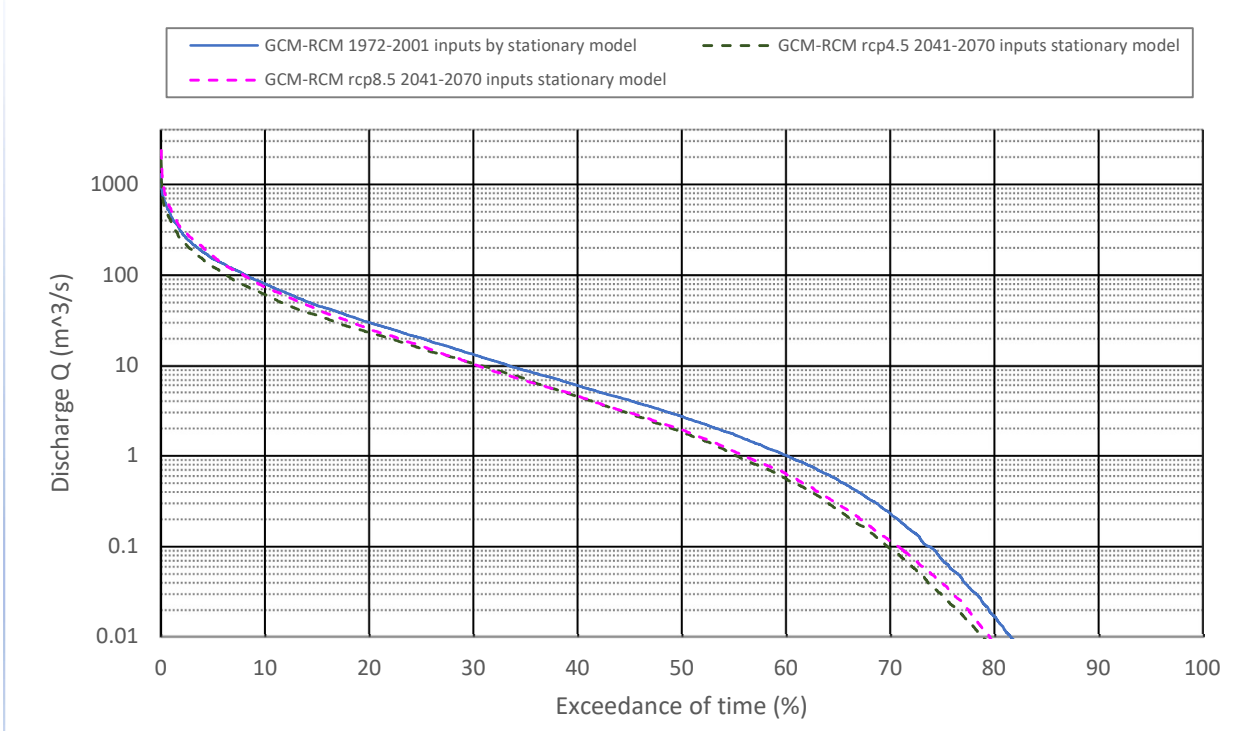
GCM-RCM 1972-2001 inputs by stationary model
GCM-RCM rcp4.5 2041-2070 inputs stationary model
GCM-RCM rcp8.5 2041-2070 inputs stationary model
Discharge Q (m^3/s)
1000
100
10
1
0.1
0.01
0
10
20
30
40
50
60
70
80
90
100
Exceedance of time (%)

(a)

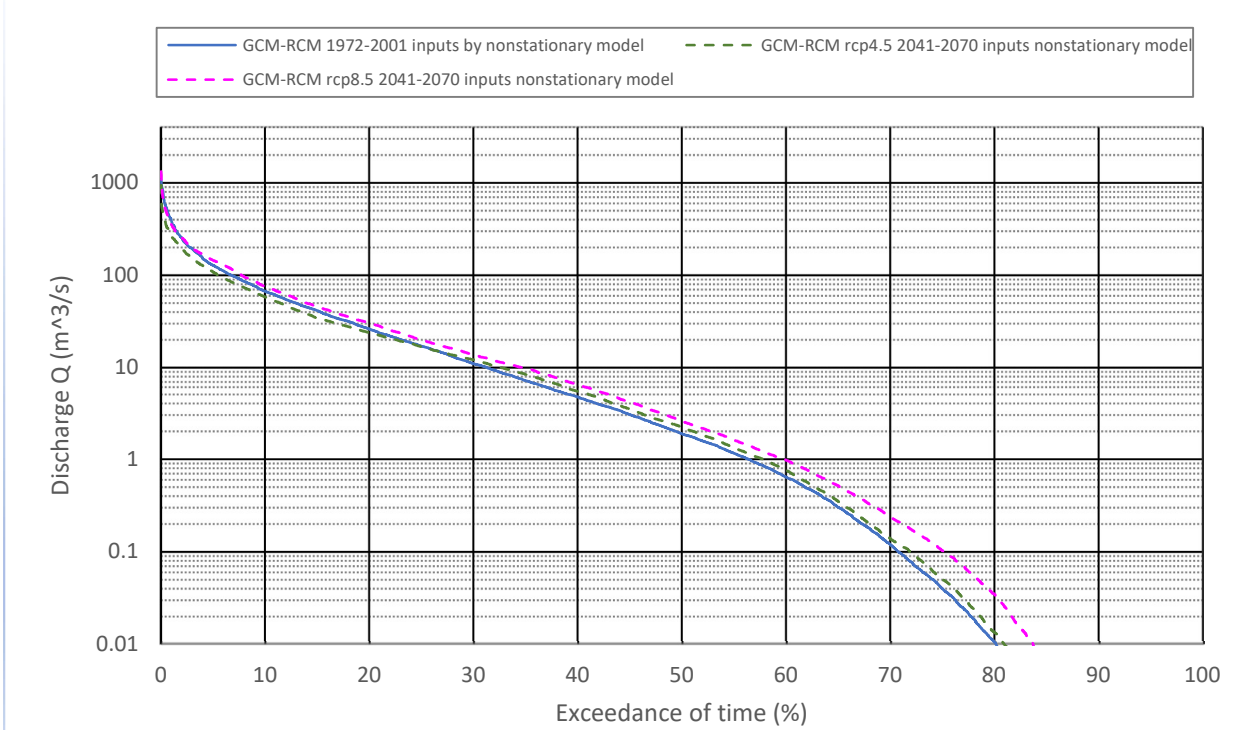
GCM-RCM 1972-2001 inputs by nonstationary model
GCM-RCM rcp4.5 2041-2070 inputs nonstationary model
GCM-RCM rcp8.5 2041-2070 inputs nonstationary model
Discharge Q (m^3/s)
1000
100
10
1
0.1
0.01
0
10
20
30
40
50
60
70
80
90
100
Exceedance of time (%)

(b)

Figure 4.6 Flow duration curves of (a): simulated discharge by stationary model with GCM-RCM historical inputs and with GCM-RCM rcp4.5 and rcp8.5 inputs for period 2045-2065; (b): simulated discharge by nonstationary model with GCM-RCM historical inputs and with GCM-RCM rcp4.5 and rcp8.5 inputs for period 2045-2065.

In Figure 4.6 (a), for the simulations with the stationary model, the flow duration curves of simulated discharges based on three input sources are close to each other. The simulated discharges based on the GCM-RCM rcp8.5 projection seems to have a smaller change to simulated discharge based on GCM-RCM historical projection, up to an exceedance frequency of only 5% are higher than simulated discharges based on GCM-RCM historical inputs, and above exceedance frequency of 5% are lower than simulated discharges based on GCM-RCM historical inputs. While the flow duration curve of simulated discharges based on the GCM-RCM rcp4.5 projection is always lower than the other two flow duration curves. The average simulated discharge with GCM-RCM historical driven inputs is about 30 m^3/s, while the average simulated discharges with GCM-RCM rcp4.5 and rcp8.5 driven inputs are 25 m^3/s and 32 m^3/s, respectively. This indicates that although up to about 95% of exceedance frequency the simulated discharges with GCM-RCM rcp8.5 are higher than simulated discharge with GCM-RCM historical inputs, the average daily discharge with GCM-RCM rcp8.5 is still lower than the average daily discharge with GCM-RCM historical inputs due to lower simulated high flows. In Figure 4.6 (b), for the simulations with the nonstationary model, the model with GCM-RCM rcp8.5 inputs simulates larger change in average flow (28 m^3/s) but with GCM-RCM rcp4.5 inputs simulates smaller change in average flow (21 m^3/s) compared to the average flow (26 m^3/s) with GCM-RCM historical inputs.

From Table 4.14 and Figure 4.6, for the period of 2045-2065, the nonstationary model simulates a lower runoff than the stationary one under each future scenario. For both stationary and nonstationary models, the simulated discharge with the GCM-RCM rcp4.5 projection as inputs shows a larger decrease in annual discharge and the simulated discharge with the GCM-RCM rcp8.5 projection as inputs shows a small increase in annual discharge compared to simulated discharge with GCM-RCM historical projection as inputs. Therefore, climate change has a large negative impact on runoff when predicting with the GCM-RCM rcp4.5 projection and has a small positive impact on runoff when predicting with the GCM-RCM rcp8.5 projection for the period of 2045-2065.

The period of 2075-2095

In Table 4.15 (a), for simulations with the stationary model, the simulated discharges with GCM-RCM rcp4.5 and rcp8.5 projections increase in spring, summer and winter but only decrease in autumn compared to simulated discharges with GCM-RCM historical inputs. The annual runoff simulated by the stationary model with GCM-RCM rcp4.5 inputs decreases but the annual runoff simulated with GCM-RCM rcp8.5 inputs increases greatly compared to the annual runoff simulated with GCM-RCM historical inputs. This happens mostly due to the less runoff from GCM-

RCM rcp4.5 than runoff from GCM-RCM rcp8.5 in all seasonal flows. For the simulations with the nonstationary model, especially for the annual runoff, the model with GCM-RCM rcp4.5 inputs simulates a decrease while the model with GCM-RCM rcp8.5 inputs shows a large increase compared to the baseline. No matter for stationary model or for nonstationary model, the annual runoff increases greatly with GCM-RCM rcp8.5 inputs and decreases slightly with GCM-RCM rcp4.5 inputs compared to the annual runoff with GCM-RCM historical inputs.

Table 4.15 Seasonal and annual difference of simulated discharges with GCM-RCM historical projection as inputs and simulated discharges with GCM-RCM rcp4.5 and rcp8.5 projections as inputs for the period of 2075-2095 with stationary and nonstationary model. The baselines are simulated discharges based on GCM-RCM historical inputs by stationary and nonstationary model, respectively.

Q (mm)	MAM		JJA		SON		DJF		Annual	
Baseline	μ	σ	μ	σ	μ	σ	μ	σ	μ	σ
GCM-RCM hist-s	0.93	0.45	0.45	0.47	0.33	0.36	0.46	0.35	0.54	0.19
	μ	σ	μ	σ	μ	σ	μ	σ	μ	σ
rcp4.5-2071-2100-s	0.94	0.56	0.47	0.39	0.21	0.33	0.51	0.34	0.53	0.20
Difference(%)	1.72	24.50	3.21	-17.11	-37.37	-6.77	10.22	-3.64	-2.15	4.75
rcp8.5-2071-2100-s	0.94	0.57	0.62	0.43	0.30	0.35	0.69	0.41	0.64	0.23
Difference(%)	2.05	26.63	36.58	-9.47	-8.36	-2.56	49.42	18.13	17.58	16.80
Baseline	μ	σ	μ	σ	μ	σ	μ	σ	μ	σ
GCM-RCM hist-ns	0.87	0.44	0.41	0.44	0.30	0.34	0.29	0.31	0.47	0.18
	μ	σ	μ	σ	μ	σ	μ	σ	μ	σ
rcp4.5-2071-2100-ns	0.92	0.55	0.44	0.38	0.18	0.30	0.28	0.25	0.46	0.19
Difference(%)	4.95	26.62	7.47	-14.58	-40.23	-13.12	-2.74	-18.94	-2.79	4.36
rcp8.5-2071-2100-ns	0.92	0.52	0.55	0.38	0.27	0.31	0.44	0.32	0.55	0.22
Difference(%)	5.14	18.31	33.87	-14.40	-7.43	-7.45	50.51	2.31	16.43	18.13

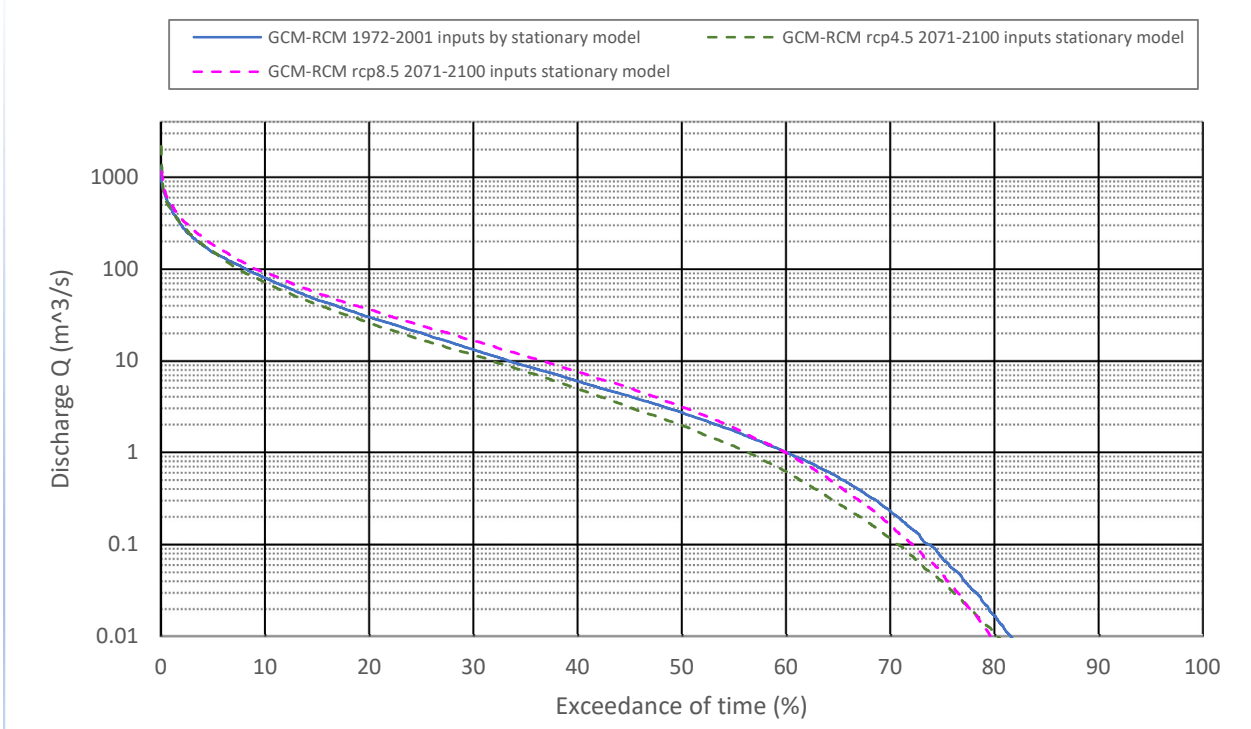

(a)

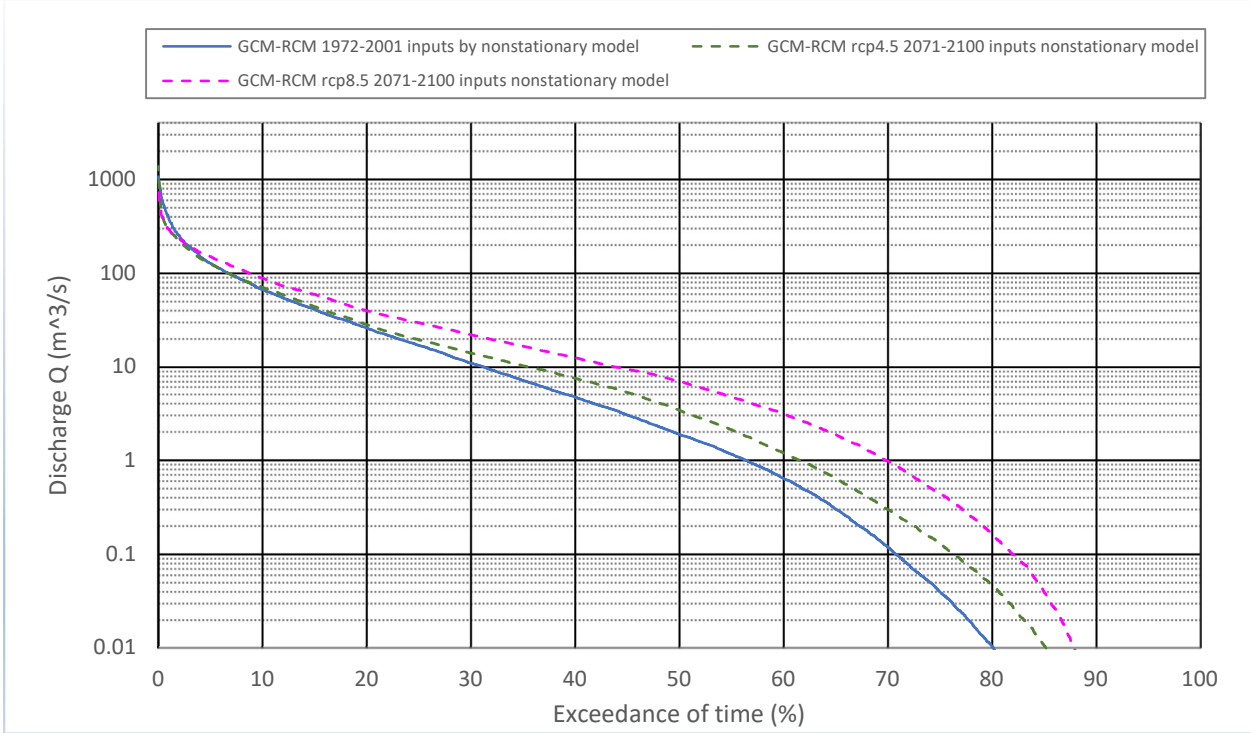

(b)

Figure 4.7 Flow duration curves of (a): simulated discharge by stationary model with GCM-RCM historical inputs and with GCM-RCM rcp4.5 and rcp8.5 inputs for period 2075-2095 and (b): simulated discharge by nonstationary model with GCM-RCM historical inputs and with GCM-RCM rcp4.5 and rcp8.5 inputs for period 2075-2095.

In Figure 4.7 (a), for simulations with the stationary model, the model with GCM-RCM rcp4.5 inputs simulates a smaller negative change in average flow (about 30 m^3/s) while the model with GCM-RCM8.5 simulates a larger positive change in average flow (about 36 m^3/s) compared to the average flow (about 30 m^3/s) simulated with GCM-RCM historical inputs. The simulated discharges with GCM-RCM rcp4.5 inputs with higher exceedance frequency than about 80% are higher than simulated discharges with GCM-RCM historical inputs while simulated discharges with GCM-RCM rcp8.5 inputs with higher exceedance frequency than about 95% are higher than simulated discharges with GCM-RCM historical inputs, this can be reflected by the values of the average annual flows. In Figure 4.7 (b), for simulations with nonstationary model, flow duration curves show that the simulated discharge with GCM-RCM rcp4.5 inputs has a smaller change in annual flow (25 m^3/s) and the simulated discharge with GCM-RCM8.5 inputs has a larger change in annual flow (about 30 m^3/s) compared to the annual flow (26 m^3/s) simulated with GCM-RCM historical inputs.

In conclusion, with inputs from each future scenario, the nonstationary model simulates less annual runoff than the stationary model. Climate change has a small negative impact on annual

runoff when predicting with GCM-RCM rcp4.5 projections and has a large positive impact on annual runoff when predicting with GCM-RCM rcp8.5 projections for the period of 2075-2095.

Chapter 5

Discussion

5.1 Regression equations

5.1.1 Sensitivity analysis

In this study, the univariate sensitivity analysis shows that the sensitivities between all four parameters and model output are similar around the optimized point where all four parameters are optimized at the same time for the whole calibration period. We assume that climate change impact on climatic characteristics can affect the optimal parameter values for hydrological models, which further influence the model output. Theoretically, due to the similar sensitivity of four parameters, every parameter should pick up significant correlations with several climatic characteristics. Based on the results of Pearson and single linear analysis, there are no significant correlations between parameter X_2 (mm/d) or X_3 (mm) and any climatic characteristics, this seems unnormal. Besides, the optimal parameter values of X_3 (mm) are extremely low in each calibration, and they are out of the 80% confidence interval of the parameter range.

However, it is thought to be not so perfect when only executing univariate sensitivity analysis to analyze sensitivity of model parameters (e.g. Tillaart, 2010). Other methods for sensitivity analysis may lead to different results, such as the Sobol's method (Pappenberger et al., 2008) and identifiability analysis (e.g. Abebe et al., 2010), etc. Comparing the results of different sensitivity analysis methods is subjective and time consuming. Therefore, univariate sensitivity analysis is used. But for further study, other methods can be executed to compare the results.

5.1.2 Regression equations

Based on the results of determining the correlations between the climatic characteristics and parameters, it is reasonable to abandon insignificant climatic characteristics and pick up statistically significant climatic characteristics to determine regression equations for optimal model parameter values. As both parameters X_1 (mm) and X_4 (d) have more than one significant climatic characteristics, multiple linear regression analysis is more suitable for determine regression equations although it might happen that only one climatic characteristic is included in one equation. The method for drawing the regression equations for both parameters is described in Chapter 3. However, it might be overparameterized because all significant climatic characteristics are put together at the beginning. But a fact is that the regression strength R^2

increases with the decrease of number of climatic characteristics in the equation, the regression equations are selected with highest value of regression strength. The difference of the method for determining regression equations from Knoben's method is that Knoben tested variety of regression equations including different number of significant climatic characteristics (see, Knoben, 2013). The regression equation with the highest value of objective function in the validation period is used for estimating that parameter value. However, that method in Knoben's study might not result in best goodness-of-fit regression equation because for specific regression equation, it might neglect some climatic characteristics which are important for determining the best regression equations for optimal parameter values. But in the other hand, with Knoben's method, overparameterization might be avoided to some extent.

A big challenge to determine the final regression equations is to redetermine regression equations based on the preliminary ones. The method is described in Chapter 3. There is a delicate relationship between the recalibrated X_2 (mm/d) and X_3 (mm) and new regression equations for parameters X_1 (mm) or X_4 (d). The new regression equations seem still to be influenced by recalibrated parameters because during recalibration, the previous regression equations were still used to determine the temporary fixed parameters. But we cannot repeat the steps to determine new regression equations again and again, and then reduce the influence of fixed parameters. Better methods to determine regression equations need to be studied in further study. In recommendation, there are some methods which can determine the regression equations for optimal parameter values.

Still, even with the new regression equations, the validation performance is still not good enough with relatively low KGE values. Therefore, it seems that the regression equations are not that robust to estimate parameter values in the validation period, and not that robust to connect model parameter values with climatic characteristics.

5.2 Climate change impact assessment

Which model is more robust for simulation

When determining the influence of the hydrological model, simulated discharges by both models with observations as inputs are compared with observed discharges. Results show that the stationary model performs better than nonstationary model, with a better KGE value (0.81 compared to 0.70). However, as the climatic characteristics are expected to influence the parameter values with climate change impacts, the nonstationary model is expected to give a better simulation than the stationary model. When determining the influence of combination of GCM-RCM projection and hydrological model, the nonstationary model shows better simulation than stationary model, with closer seasonal and annual flows compared to observed flows, this seems to meet expectation.

Difference of climate change impact on runoff in different future periods

An interesting result is that in the future period of 2045-2065, climate change has more impact on runoff predicted with GCM-RCM rcp4.5 than with GCM-RCM rcp8.5. While in the future period of 2075-2095, climate change has more impact on runoff predicted with GCM-RCM rcp8.5 than with GCM-RCM rcp4.5. This tendency also suits for P and PET, but climate change has more impact on T when predicting with rcp8.5 than with rcp4.5 for both periods. It is not clear whether the change of inputs P and PET affect output more than the change of input T in modeling only based on the results described above. However, it seems interesting to execute further study to verify if this is correct.

Totally, the conclusion seems that for different study catchments with different datasets, it is to be tested and considered that either stationary model or non-stationary model is robust for simulation under historical and future conditions. In this study, the climate change impacts on runoff are different with different models even under the same period, but it is still not good prediction with either of models. The climate change impact assessment on future runoff with a specific hydrological model seems reliable only when the model simulates runoff with small bias compared to historical observed runoff.

Chapter 6

Conclusions and recommendations

6.1 Conclusions

Firstly, this study aims to establish relationships between model parameters and climatic characteristics and quantify how the relationships perform during validation. Secondly, with the results, the objective is to assess whether either the stationary model or non-stationary model can give better runoff simulations in historical period, and then assess climate change impact on runoff in future periods with both models.

Pearson correlations between optimized four parameters and 18 climatic characteristics have been assessed, firstly. With single linear regression analysis, significant correlations between model parameters and climatic characteristics are determined. Results show that there are no significant correlations between parameters X_2 (mm/d) and X_3 (mm) and any climatic characteristics. Parameter X_1 (mm) has significant correlations with 4 climatic characteristics, while parameter X_4 (d) has significant correlations with 9 climatic characteristics with different single linear regression strength R^2. Based on significant climatic characteristics, multiple regression equations are determined for X_1 (mm) and X_4 (d).

The reverse order for calibration and validation is done to determine which period is more suitable to establish regression equations and then assess climate change impact. The results show that with sequential order of calibration and validation, the determined regression equations can result in higher KGE values (0.80 for calibration and 0.66 for validation) than with reverse order (0.81 for calibration and 0.64 for validation). Therefore, hydrological simulations incorporating parameter non-stationarity with the regression equations for parameters X_1 (mm) and X_4 (d) from the sequential order of calibration and validation are done in assessing simulation performance by non-stationary model.

Due to the bias in GCM-RCM historical projection and differences in GCM-RCM future projections of precipitation, temperature and calculated potential evapotranspiration compared to observations and GCM-RCM historical inputs, respectively, the regression equations for parameters X_1 (mm) and X_4 (d) perform unsatisfactory due to the low values of the objective function. Both parameter values of X_1 (mm) and X_4 (d) show an increasing tendency, especially for X_4 (d).

Under each simulation period either historical period or future periods, the simulated average discharge by non-stationary model is lower than the simulated average discharge by stationary

model. With observed inputs, the simulated extreme high flows simulated by the stationary model are similar than by the non-stationary model, With GCM-RCM projected inputs from both historical and future periods, the simulated extreme high flows simulated by the stationary model are much higher (up to 54%) than the extreme high flows simulated by the non-stationary model. From the results, it does indicate that non-stationarity in models may have huge effects on climate change impacts while at the same time time-window calibration does show that optimal parameter values do vary in time in somewhat hydro-climatically interpretable ways.

Comparing the influence of hydrological models, the stationary model with observed inputs performs better than the nonstationary model with observed inputs compared to observed discharge and simulates higher seasonal and annual flow than the nonstationary model. Both models underestimate annual flow compared to observed annual flow. When comparing the influence of GCM-RCM historical projection, both models show that simulated discharges with GCM-RCM historical projection as inputs are much higher than simulated discharges with observations as inputs in spring, summer, winter and annually. This is mostly due to the higher estimation of precipitation and lower estimation of potential evapotranspiration from GCM-RCM historical projection than observed precipitation and calculated potential evapotranspiration. When comparing the influence of GCM-RCM combinations and hydrological models, the nonstationary model seems to perform better than the stationary model with a closer estimation of annual flow compared to observed annual flow. However, both models overestimate annual flows compared to observed annual flow. Totally, non-stationary model incorporating regression equations for optimal parameters is more accurate when applying the GR4J hydrological model in runoff simulation with GCM-RCM historical projection, and more recommended for climate change impact assessment on runoff when using the same GCM-RCM combination with future projections.

In both future periods, both models show decreased annual flows with GCM-RCM rcp4.5 projection as inputs and increased annual flows with GCM-RCM rcp8.5 projection as inputs. In the first period for 2045-2065, however, stationary and non-stationary model simulates higher discharges (7% and 6%, respectively) with GCM-RCM rcp8.5 projection and lower discharges (18% and 19%, respectively) with GCM-RCM rcp4.5 projection than discharges with GCM-RCM historical projection. Therefore, climate change impact will result in a large decrease in runoff with GCM-RCM rcp4.5 projection and a small increase in annual runoff with GCM-RCM rcp8.5 projection compared to the annual runoff with GCM-RCM historical projection. While in the second period for 2075-2095, stationary and non-stationary model simulates lower discharges (2% and 3%, respectively) with GCM-RCM rcp4.5 projection and higher discharges (18% and 16%, respectively) with GCM-RCM rcp8.5 projection than discharges simulated with GCM-RCM historical projection. Therefore, climate change impact will result in a small decrease in annual runoff change with GCM-RCM rcp4.5 projection and a large increase in annual runoff change with GCM-RCM rcp8.5 projection than the annual runoff with GCM-RCM historical projection.

6.2 Recommendations

For further research to study relationship between model parameters and climatic characteristics and assess climate change impacts on runoff with stationary and non-stationary models, the following recommendations are proposed:

1. This study only uses one objective function to show model performance compared with observed runoff. However, different objective functions will lead to different comparison results, and therefore maybe different conclusions. Therefore, using combination of objective functions may avoid the domain of results by one objective function. For example, compare the results of values of objective functions NS and RVE in the validation period, the optimal NS value is 1, and he optimal RVE value is 0.
2. In this study, the GR4J rainfall-runoff model with four parameters is used. In the determination of the regression equations, parameters X_2 (mm/d) and X_3 (mm) have fixed values. This eliminates interactions between fixed parameters and non-stationary parameters, and this seems unwise. Because the optimal parameter values are expected to change in different simulation periods within the non-stationary model, even for the parameters which cannot be determined with significant climatic characteristics. Therefore, taking X_2 (mm/d) and X_3 (mm) as stable values will affect the optimization of X_1 (mm) and X_4 (d) due to interactions of parameters. Besides, other relationships for the fixed parameters may exist, for example, relationships between 'fixed' parameters and 'non-stationary' parameters. In further study, it is recommended to explore the potential relationships between the 'fixed' parameters (if there are) and 'non-stationary' parameters and apply the relationships in the determination of 'non-stationary' parameter values.
3. In the process of determining regression equations, recalibration is done to redetermine the equation set. As discussed in section 5.1.2, the influence from fixed parameters cannot be eliminated completely in determine new regression equation set. The first recommendation is to repeat the steps described in methodology to reduce the influence of fixed parameters in determination of equations. The second recommendation is to use the firstly determined regression equations, as optimal parameters change in each simulation period, the determined equations are just from the non-stationary optimal parameters. Recalibration is for making parameters with no significant correlations (so called fixed parameters) compatible with parameters with significant correlations (so called non-stationary parameters). The results from the second recommendation is the first regression equations obtained in section 4.3.3. The third recommendation is to use the calibrated results in stationary case as the stable parameter values. For example, in this study, the values of X_2 (mm/d) and X_3 (mm) are fixed values obtained in stationary calibration, then only X_1 (mm) and X_4 (d) are calibrated in each 10-year time window. Then the optimized parameters are used to determine regression equation set. Besides, in this study, the regression equations use all significant climatic characteristics at the

beginning, however, this may result in overparameterization. Therefore, it is recommended to analyze the hydrological relations between the significant climatic characteristics and the parameters at first, then test the regression equations determined with the hydrologically significant climatic characteristics for optimal parameters to see which one has the highest value of regression strength R^2, this may avoid the overparameterization to some extent.

4. In the results of climate change impact assessment, we found that for both models, climate change has more impacts on runoff when predicting with GCM-RCM rcp4.5 than with GCM-RCM rcp8.5 in the future period of 2045-2065, but has more impacts on runoff when predicting with GCM-RCM rcp8.5 than with GCM-RCM rcp4.5 in the future period of 2075-2095. A similar trend is found in the climate change impacts on P and PET, but climate change has more impact on T for both future periods from GCM-RCM rcp4.5 and rcp8.5. Therefore, it is recommended to do further study to explore if the change of P and PET as model inputs affect output more than the change of T as model inputs.
5. This study has selected the gridded solution '22i' for calculating model inputs for this catchment. The alternative selections may be the gridded solution '11i' or '44i'. However, for large catchment, the gridded solution '44i' is not recommended due to lack of precise. It is certain that using gridded solution '11i' can lead to more precise calculating but need more work and time. Therefore, gridded solution '11i' is recommended in further study when using catchments scale like this catchment or larger catchment scales.

References

Abebe, N. A., Ogden, F. L., & Pradhan, N. R. (2010). Sensitivity and uncertainty analysis of the conceptual HBV rainfall–runoff model: Implications for parameter estimation. *Journal of Hydrology*, *389*(3-4), 301-310.

Akhtar, M., Ahmad, N., & Booij, M. J. (2009). Use of regional climate model simulations as input for hydrological models for the Hindukush-Karakorum-Himalaya region. *Hydrology and Earth System Sciences*, *13*(7), 1075.

Allen, R. G., Pereira, L. S., Raes, D., & Smith, M. (1998). Crop evapotranspiration-Guidelines for computing crop water requirements-FAO Irrigation and drainage paper 56. *Fao, Rome*, *300*(9), D05109.

Andréassian, V., Perrin, C., Michel, C., Usart-Sanchez, I., & Lavabre, J. (2001). Impact of imperfect rainfall knowledge on the efficiency and the parameters of watershed models. *Journal of Hydrology*, *250*(1-4), 206-223.

Baez-Villanueva, O. M., Zambrano-Bigiarini, M., Ribbe, L., Nauditt, A., Giraldo-Osorio, J. D., & Thinh, N. X. (2018). Temporal and spatial evaluation of satellite rainfall estimates over different regions in Latin-America. *Atmospheric Research*, *213*, 34-50.

Bastola, S., Murphy, C., & Sweeney, J. (2011). Evaluation of the transferability of hydrological model parameters for simulations under changed climatic conditions. *Hydrology and Earth System Sciences Discussions*, *8*, 5891-5915.

Blazs, R. L., Walters, D. M., Coffey, T. E., Boyle, D. L., & Wellman, J. J. (2003). Water resources data, Oklahoma, water year 2000. *Red River basin and ground-water wells: US Geological Survey Water-Data Report OK-02-2*.

Booij, M. J. (2005). Impact of climate change on river flooding assessed with different spatial model resolutions. *Journal of hydrology*, *303*(1-4), 176-198.

Booij, M. J., Tollenaar, D., van Beek, E., & Kwadijk, J. C. (2011). Simulating impacts of climate change on river discharges in the Nile basin. *Physics and Chemistry of the Earth, Parts A/B/C*, *36*(13), 696-709.

Cannon, A. J. (2018). Multivariate quantile mapping bias correction: an N-dimensional probability density function transform for climate model simulations of multiple variables. *Climate dynamics*, *50*(1-2), 31-49.

Chattopadhyay, N., & Hulme, M. (1997). Evaporation and potential evapotranspiration in India under conditions of recent and future climate change. *Agricultural and Forest Meteorology*, *87*(1), 55-73.

Chiew, F. H. S., Teng, J., Vaze, J., Post, D. A., Perraud, J. M., Kirono, D. G. C., & Viney, N. R. (2009). Estimating climate change impact on runoff across southeast Australia: Method, results, and implications of the modeling method. *Water Resources Research*, *45*(10).

Coron, L., Andreassian, V., Perrin, C., Lerat, J., Vaze, J., Bourqui, M., & Hendrickx, F. (2012). Crash testing hydrological models in contrasted climate conditions: An experiment on 216 Australian catchments. *Water Resources Research*, *48*(5).

Davis, J.C. (2002), *Statistics and Data Analysis in Geology*, 3rd edition. John Wiley and Sons, New York, NY, USA.

Dumouchel, W., & O'Brien, F. (1989, April). Integrating a robust option into a multiple regression computing environment. In *Computer science and statistics: Proceedings of the 21st symposium on the interface* (pp. 297-302). American Statistical Association Alexandria, VA.

Edijatno, N., & Michel, C. (1989). Un modèle pluie-débit journalier à trois paramètres. *La Houille Blanche*, *2*, 113-121.

El-Nasr, A. A., Arnold, J. G., Feyen, J., & Berlamont, J. (2005). Modelling the hydrology of a catchment using a distributed and a semi-distributed model. *Hydrological Processes: An International Journal*, *19*(3), 573-587.

Franco, A. C. L., & Bonumá, N. B. (2017). Multi-variable SWAT model calibration with remotely sensed evapotranspiration and observed flow. *RBRH*, *22*.

Gupta, H. V., Kling, H., Yilmaz, K. K., & Martinez, G. F. (2009). Decomposition of the mean squared error and NSE performance criteria: Implications for improving hydrological modelling. *Journal of hydrology*, *377*(1-2), 80-91.

Hargreaves, G. H., & Samani, Z. A. (1985). Reference crop evapotranspiration from temperature. *Applied engineering in agriculture*, *1*(2), 96-99.

Holland, P. W., & Welsch, R. E. (1977). Robust regression using iteratively reweighted least-squares. *Communications in Statistics-theory and Methods*, *6*(9), 813-827.

Huber, P. J. Robust Statistics. Hoboken, NJ: John Wiley & Sons, Inc., 1981.

Knoben, W. J. M. (2013). *Estimation of non-stationary hydrological model parameters for the Polish Welna catchment* (Master's thesis, University of Twente).

Kim, K. B., Kwon, H. H., & Han, D. (2018). Exploration of warm-up period in conceptual hydrological modelling. *Journal of Hydrology*, *556*, 194-210.

Lindström, G., Johansson, B., Persson, M., Gardelin, M., & Bergström, S. (1997). Development and test of the distributed HBV-96 hydrological model. *Journal of hydrology*, *201*(1-4), 272-288.

Mearns, L.O., et al., 2017: *The NA-CORDEX dataset*, version 1.0. NCAR Climate Data Gateway, Boulder CO, accessed [date], https://doi.org/10.5065/D6SJ1JCH.

Merz, R., Parajka, J., & Blöschl, G. (2009). Scale effects in conceptual hydrological modeling. *Water resources research*, *45*(9).

Merz, R., Parajka, J., & Blöschl, G. (2011). Time stability of catchment model parameters: Implications for climate impact analyses. *Water Resources Research*, *47*(2).

MOPEX data sets are available at: https://hydrology.nws.noaa.gov/pub/gcip/mopex/US_Data/.

Nash, J. E., & Sutcliffe, J. V. (1970). River flow forecasting through conceptual models part I—A discussion of principles. *Journal of hydrology*, *10*(3), 282-290.

N. O. Nascimento," *Appreciation a L'aide D'un Modele Emirique Des Effets D'action Anthropiques Sur La Relation Pluie-Debit a L'echelle Du Bassin Versant*", PhD Thesis, CERGRENE/ENPC, Paris, France, 1995, 550 pp.

Ouarda, T. B., Charron, C., & St-Hilaire, A. (2020). Uncertainty of stationary and nonstationary models for rainfall frequency analysis. *International Journal of Climatology*, *40*(4), 2373-2392.

Pappenberger, F., Beven, K. J., Ratto, M., & Matgen, P. (2008). Multi-method global sensitivity analysis of flood inundation models. *Advances in water resources*, *31*(1), 1-14.

Pechlivanidis, I. G., Jackson, B. M., Mcintyre, N. R., & Wheater, H. S. (2011). Catchment scale hydrological modelling: a review of model types, calibration approaches and uncertainty analysis methods in the context of recent developments in technology and applications. *Global NEST journal*, *13*(3), 193-214.

Perrin, C., Michel, C., & Andréassian, V. (2003). Improvement of a parsimonious model for streamflow simulation. *Journal of hydrology*, *279*(1-4), 275-289.

Pool, S., Vis, M., & Seibert, J. (2018). Evaluating model performance: towards a non-parametric variant of the Kling-Gupta efficiency. *Hydrological sciences journal*, *63*(13-14), 1941-1953.

Schaake, J., Cong, S., & Duan, Q. (2006). The US MOPEX data set. *IAHS publication*, *307*(9).

Schipper, T. C. (2017). *The attribution of changes in streamflow to climate and land use change for 472 catchments in the United States and Australia* (Master's thesis, University of Twente).

Seibert, J. (2003). Reliability of Model Predictions Outside Calibration Conditions: Paper presented at the Nordic Hydrological Conference (Røros, Norway 4-7 August 2002). *Hydrology Research*, *34*(5), 477-492.

Sepaskhah, A. R., & Razzaghi, F. (2009). Evaluation of the adjusted Thornthwaite and Hargreaves-Samani methods for estimation of daily evapotranspiration in a semi-arid region of Iran. *Archives of Agronomy and Soil Science*, *55*(1), 51-66.

Smith, J. B., Schneider, S. H., Oppenheimer, M., Yohe, G. W., Hare, W., Mastrandrea, M. D., ... & Füssel, H. M. (2009). Assessing dangerous climate change through an update of the Intergovernmental Panel on Climate Change (IPCC)“reasons for concern”. *Proceedings of the national Academy of Sciences*, *106*(11), 4133-4137.

Spencer, J. W. (1971). Fourier series reprensentation of the position of the sun. *Search*, *2*(5), 172.

Street, J. O., Carroll, R. J., & Ruppert, D. (1988). A note on computing robust regression estimates via iteratively reweighted least squares. *The American Statistician*, *42*(2), 152-154.

Tian, Y., Xu, Y. P., & Zhang, X. J. (2013). Assessment of climate change impacts on river high flows through comparative use of GR4J, HBV and Xinanjiang models. *Water resources management*, *27*(8), 2871-2888.

Tillaart, S. P. (2010). *Influence of uncertainties in discharge determination on the parameter estimation and performance of a HBV model in Meuse sub basins* (Master's thesis, University of Twente).

Trucano, T. G., Swiler, L. P., Igusa, T., Oberkampf, W. L., & Pilch, M. (2006). Calibration, validation, and sensitivity analysis: What's what. *Reliability Engineering & System Safety*, *91*(10-11), 1331-1357.

Wheater, H. S. (2002). Progress in and prospects for fluvial flood modelling. *Philosophical Transactions of the Royal Society of London. Series A: Mathematical, Physical and Engineering Sciences*, *360*(1796), 1409-1431.

Woodward, A., Smith, K. R., Campbell-Lendrum, D., Chadee, D. D., Honda, Y., Liu, Q., ... & Confalonieri, U. (2014). Climate change and health: on the latest IPCC report. *The Lancet*, *383*(9924), 1185-1189.

Xu, C. Y. (1999). Operational testing of a water balance model for predicting climate change impacts. *Agricultural and forest meteorology*, *98*, 295-304.

Xu, C. Y., & Singh, V. P. (2004). Review on regional water resources assessment models under stationary and changing climate. *Water resources management*, *18*(6), 591-612.

Yin, Y., Wu, S., Chen, G., & Dai, E. (2010). Attribution analyses of potential evapotranspiration changes in China since the 1960s. *Theoretical and Applied Climatology*, *101*(1-2), 19-28.

Appendices

Appendix A

Historical and future datasets

Historical dataset

'prec. hist. CanESM2. CanRCM4. day. NAM-22i. mbcn-Daymet';

'tmax. hist. CanESM2. CanRCM4. day. NAM-22i. mbcn-Daymet';

'tmin. hist. CanESM2. CanRCM4. day. NAM-22i. mbcn-Daymet'.

Where, 'prec', 'tmax' and 'tmin' mean 'precipitation', 'maximum temperature' and 'minimum temperature', respectively. 'Hist' means historical scenario running from 1950 – 2001. 'CanESM2' and 'CanRCM4' stand for GCM and RCM, respectively. All data are simulated as daily results. 'NAM-22i' indicates 0.22°/25km native rotated-pole grids. The 'i' suffix indicates that the data has been interpolated to a common quarter lat-lon grid. As raw data are uncorrected model output, 'mbcn-Daymet' has been bias-corrected using cannon's MBCn algorithm against Daymet gridded observational datasets (Mearns et al., 2017). Notably, for this GCM-RCM projection, the calendar has 365 days in each year. The description of different variables in each dataset file is in Table A.1.

Table A.1 Description of variables in each dataset file.

Climatic characteristics	Scenario	GCM	RCM	Frequency	Grid	Bias correction
Prec	historical	CanESM2	CanRCM4	Day	NAM-22i	mbcn-Daymet
Tmax	historical	CanESM2	CanRCM4	Day	NAM-22i	mbcn-Daymet
Tmin	historical	CanESM2	CanRCM4	Day	NAM-22i	mbcn-Daymet
Prec	Rcp4.5	CanESM2	CanRCM4	Day	NAM-22i	mbcn-Daymet
Tmax	Rcp4.5	CanESM2	CanRCM4	Day	NAM-22i	mbcn-Daymet
Tmin	Rcp4.5	CanESM2	CanRCM4	Day	NAM-22i	mbcn-Daymet

Prec	Rcp8.5	CanESM2	CanRCM4	Day	NAM-22i	mbcn-Daymet
Tmax	Rcp8.5	CanESM2	CanRCM4	Day	NAM-22i	mbcn-Daymet
Tmin	Rcp8.5	CanESM2	CanRCM4	Day	NAM-22i	mbcn-Daymet

Future input data predictions

Future data of different climatic characteristics in North American catchments are available, based on the results of combinations of Global and Regional Climate Models with rcp4.5 and rcp8.5 scenarios (GCM and RCM, respectively). The source is also from NA-CORDEX (Mearns et al., 2017). The selected data source is:

'prec. rcp4.5. CanESM2. CanRCM4. day. NAM-22i. mbcn-Daymet';

'tmax. rcp4.5. CanESM2. CanRCM4. day. NAM-22i. mbcn-Daymet';

'tmin. rcp4.5. CanESM2. CanRCM4. day. NAM-22i. mbcn-Daymet';

'prec. rcp8.5. CanESM2. CanRCM4. day. NAM-22i. mbcn-Daymet';

'tmax. rcp8.5. CanESM2. CanRCM4. day. NAM-22i. mbcn-Daymet';

'tmin. rcp8.5. CanESM2. CanRCM4. day. NAM-22i. mbcn-Daymet'.

Where, 'rcp' means future scenario running from 2006 – 2100. For this future scenario, the calendar has 365 days in each year. The description of variables in each dataset file can be found in Table 2.1.

Appendix B

Potential evapotranspiration calculation

The provided potential evapotranspiration data in MOPEX is climatological values, which cannot be used directly for simulation. This appendix provides a method to obtain corrected potential evapotranspiration for model simulation. The equation of Hargreaves (Hargreaves & Samani, 1985) can be used to estimate daily PET. This equation is used because it only requires the minimum and maximum temperature. Equation 2 is used to correct the estimated PET values. The equations are as follows:

$$PET_{d,est} = 0.408 * 0.0023RA(\frac{T_{max} + T_{min}}{2} + 17.8)\sqrt{T_{max} - T_{min}}$$

$$PET_{d,corr} = PET_{d,est} * \frac{PET_{m\ avg,cl}}{PET_{m\ avg,est}}$$

Where $PET_{d,est}$ is the daily estimated potential evapotranspiration in mm d^{-1}, RA is the extraterrestrial radiation in MJ m^{-2} d^{-1}, T_{max} is the maximum daily temperature in degrees Celsius and T_{min} is the minimum daily temperature in degrees Celsius. The factor 0.408 is added to convert the unit from MJ m^{-2} d^{-1} to mm d^{-1}.

The climatological monthly average PET ($PET_{m\ avg,cl}$) data is needed to correct the obtained $PET_{d,est}$ (Schaake et al., 2006). A correction factor for each month will be calculated by dividing monthly average potential evapotranspiration (climatological values) by the monthly average, obtained from the estimated potential evapotranspiration ($PET_{m\ avg,est}$). This factor is used to multiply it with $PET_{d,est}$. And then the corrected daily potential evapotranspiration $PET_{d,corr}$ is obtained.

For applying the equation of Hargreaves (Hargreaves & Samani, 1985), it is needed to calculated the extraterrestrial radiation (RA) in MJ m^{-2} d^{-1}, which is a parameter indicating the intensity of the solar irradiation directly outside the earth's atmosphere (Allen et al., 1998):

$$RA = \frac{G_{sc}}{\pi} d_r * \omega_s\ sin\phi\ sin\delta + cos\phi\ cos\delta\ sin\omega_s$$

Where the inverse relative distance earth-sun (d_r) and the sunset hour angle (ω_s) are calculated by:

$$d_r = 1 + 0.033\cos(\frac{2\pi}{365}n)$$

$$\omega_s = cos^{-1}(-tan\delta\ tan\phi)$$

And G_{sc} is the solar constant, which is 118.1 MJ m^{-2} d^{-1}. The declination (δ in radians), the angel between the sun and the earth's equator is calculated by the following equation (Spencer, 1971):

$$\delta = 0.006918 - 0.399912\ cosB + 0.070257\ sinB - 0.006758\ cos2B + 0.000907\ sin2B - 0.002697\ cos3B + 0.001480\ sin3B$$

Where:

$$B = (n-1)\frac{360}{365}$$

at the n^{th} day of the year. The number 365 indicates the number of days in a year, so days in a leap year will be calculated by making use of 366 instead of 365 (for historical data, for future data, it is always 365). This also holds for equation of d_r. For latitudes (L) in decimal degrees, the next equation will be used for translating to radials:

$$\phi = L * \frac{\pi}{180}$$

Where ϕ is latitude in radials, which makes it applicable for substituting in equations of RA and ω_s, respectively.

Appendix C

Multiple linear regression analysis

This appendix describes the determination process of multiple linear regression, this regression uses model parameter values obtained by calibrating all four parameters in each of 20 10-year time windows. The values of the optimized parameter values can be found in Table C.1.

Table C.1 Optimized parameter values for each of 20 10-year time windows.

10-year time window	X_1 (mm)	X_2 (mm/d)	X_3 (mm)	X_4 (d)
1949-1958	133.64	-0.00	0.00	2.61
1950-1959	123.80	-0.00	0.00	2.66
1951-1960	113.68	-0.00	0.00	2.72
1952-1961	141.37	-0.01	0.01	2.60
1953-1962	143.25	-0.00	0.00	2.60
1954-1963	149.99	-0.00	0.00	2.81
1955-1964	124.79	-0.05	0.05	2.50
1956-1965	123.39	-0.00	0.00	2.50
1957-1966	124.44	-0.01	0.00	2.50
1958-1967	130.90	-0.00	0.00	2.43
1959-1968	110.65	-0.00	0.00	2.47
1960-1969	101.26	-0.09	0.12	2.38
1961-1970	99.27	-0.35	0.78	2.23
1962-1971	111.05	-0.45	1.06	2.14
1963-1972	101.01	-0.87	2.26	2.08
1964-1973	96.40	-0.50	1.09	2.22
1965-1974	107.68	-0.29	0.52	2.28
1966-1975	104.69	-0.29	0.58	2.30
1967-1976	110.37	-0.22	0.38	2.29
1968-1977	125.76	-0.07	0.08	2.32

Regression equation for X_1 (mm)

With Mat-Lab functions '$fitlm$' and '$anova$', the table including each significant climatic characteristic and their relevant significance levels (p-value) can be obtained, the regression strength R^2 is also available for adjudging if the regression equation becomes better by deleting 'insignificant' variables one by one. The results are shown as follows from Table C.2.

Table C.2 (a) to Table C.2 (e) show the process of determining regression equation for model parameter X_1 (mm). Table C.2 (a) shows the all the significant climatic variables in the regression equation with the regression strength R^2 = 0.35. Obviously, due to the interactions of climatic characteristics, the climatic characteristics with the coefficients are no significant at 95% level anymore. The solution should be deleting one climatic variable with the highest p-value in the regression equation by Mat-Lab fuction '$removeTerms$'. Therefore, the climatic variable with coefficient C_2 is removed according to Table C.2 (a). Then Table C.2 (b) is obtained. The regression strength R^2 of the regression equation with 4 coefficients increases 0.02 comparing with the regression equation with 5 coefficients. Next, the climatic variable with coefficient C_1 is removed, the result is shown in Table C.2 (c). The regression strength R^2 becomes 0.39 when the regression equation includes 3 coefficients. Last, the climatic variable with coefficient C_4 is removed, the regression equation for X_1 (mm) is obtained with all included climatic variables having p-values less than 0.05, the results are shown in Table C.2 (d). To verify if this is the best regression equation, the constant C_0 is removed, the results are shown in Table C.2 (e), the regression strength R^2 decreases a lot with a value 0.01. Therefore, the final regression equation for X_1 (mm) is determined by Table C.2 (d) with the highest regression strength R^2 = 0.40. The regression equation is expressed as:

$$X_1 = -768.40 + 83.74 * T_{sd}$$

Table C.2 Determination process of multiple linear regression equation for parameter X_1 (mm) from (a) to (e). C_n are the coefficients of significant climatic variables, p-value shows the significance level of each climatic variable in the regression equation, and R^2 shows the regression strength of the regression equation.

(a)

	Coefficients	p-value	R^2
C_0	-402.41	0.56	0.35
C_1	-376.01	0.35	
C_2	54.96	0.49	
C_3	33.36	0.44	
C_4	30.77	0.28	

(b)

	Coefficients	p-value	R^2
C_0	-765.63	0.09	0.37
C_1	-152.79	0.52	
C_3	53.38	0.10	
C_4	34.23	0.21	

(c)

	Coefficients	p-value	R^2
C_0	-965.31	0.00	0.39

C_3	56.13	0.08	
C_4	18.49	0.10	

(d)

	Coefficients	p-value	R^2
C_0	-768.40	0.01	0.40
C_3	83.74	0.01	

(e)

	coefficients	p-value	R^2
C_3	11.23	0.00	0.01

Regression equation for X_4 (d)

Table C.3 (a) to Table C. (i) show the process of determination of multiple linear regression equation for X_4 (d) with Mat-Lab functions '$fitlm$' and '$anova$'. The first result including all significant climatic characteristics and the regression strength R^2 is shown in Table C.3 (a). The climatic variable with coefficient C_6 has the highest p-value, thus this climatic variable should be removed first. Table C.3 (b) shows the results with 9 coefficients and their p-values, the regression strength increases to 0.56, which means the new regression equation performs better than the regression equation with all significant climatic variables. Next, according to Table C.3 (b), the climatic variables with coefficients C_7, C_8, C_9, C_4, C_0 and C_1 are removed, respectively. To compare if the regression equation has the best goodness of fit, the climatic variable with coefficient C_5 is removed although its p-value is lower than 0.05. The result show that the regression strength R^2 = 0.55 which is much lower than R^2 =0.64 resulted from regression equation with 3 climatic variables. Therefore, the final regression equation for parameter X_4 (d) is shown as:

$$X_4 = -8.39 * PET + 1.34 * T + 0.57 * T_s$$

Table C.3 Determination process of multiple linear regression equation for parameter X_4 (d) from (a) to (i). C_n are the coefficients of significant climatic variables, p-value shows the significance level of each climatic variable in the regression equation, and R^2 shows the regression strength of the regression equation.

(a)

	Coefficients	p-value	R^2
C_0	8.95	0.78	0.52
C_1	-2.18	0.39	

C_2	-11.19	0.20	
C_3	1.27	0.24	
C_4	0.86	0.40	
C_5	0.34	0.61	
C_6	0.37	0.92	
C_7	-0.20	0.73	
C_8	3.85	0.72	
C_9	-0.22	0.88	

(b)

	Coefficients	p-value	R^2
C_0	10.78	0.68	0.56
C_1	-2.25	0.34	
C_2	-11.53	0.13	
C_3	1.27	0.22	
C_4	0.80	0.32	
C_5	0.38	0.50	
C_7	-0.18	0.73	
C_8	3.56	0.72	
C_9	-0.34	0.67	

(c)

	Coefficients	p-value	R^2
C_0	13.96	0.55	0.59
C_1	-2.15	0.34	
C_2	-11.38	0.12	
C_3	1.13	0.21	
C_4	0.72	0.32	
C_5	0.43	0.40	
C_8	0.81	0.89	
C_9	-0.16	0.78	

(d)

	Coefficients	p-value	R^2
C_0	16.72	0.19	0.62
C_1	-2.38	0.11	
C_2	-12.09	0.02	
C_3	1.15	0.18	
C_4	0.65	0.21	
C_5	0.49	0.09	
C_9	-0.09	0.73	

(e)

	Coefficients	p-value	R^2
C_0	15.75	0.19	0.65
C_1	-2.16	0.09	
C_2	-11.65	0.02	
C_3	1.05	0.17	
C_4	0.63	0.21	
C_5	0.50	0.07	

(f)

	Coefficients	p-value	R^2
C_0	14.04	0.24	0.63
C_1	-1.29	0.22	
C_2	-12.53	0.01	
C_3	1.64	0.01	
C_5	0.56	0.05	

(g)

	Coefficients	p-value	R^2
C_1	-0.15	0.71	0.62
C_2	-7.92	0.00	
C_3	1.27	0.02	
C_5	0.56	0.05	

(h)

	Coefficients	p-value	R^2
C_2	-8.39	0.00	0.64
C_3	1.34	0.01	
C_5	0.57	0.04	

(i)

	Coefficients	p-value	R^2
C_2	-6.58	0.00	0.55
C_3	1.91	0.00	

Appendix D

Comparison of optimized parameters and calculated parameters with the regression equations

After the regression equations for X_1 (mm) and X_4 (d) is determined, the parameter values of X_1 (mm) and X_4 (d) in the validation period should be calculated to execute simulation and see the performance of simulation with the regression equations. The results show that the values of objective function KGE are 0.80 for calibration and 0.66 for validation. Besides, the comparison between optimized parameter values and calculated parameter values with the determined regression equations can be done to verify the accuracy of the regression equations both for calibration and validation (in Table D.1 and Figure D.1).

Table D.1 The optimized and calculated parameter values with the regression equations for X_1 (mm) and X_4 (d), (a) includes the results from the calibration period and (b) includes the results from the validation period.

(a)

10-year time windows in calibration period	Optimized		Calculated	
	X_1(mm)	X_4(d)	X_1(mm)	X_4(d)
1949-1958	97.23	2.66	104.19	2.73
1950-1959	112.69	2.68	119.13	2.66
1951-1960	107.65	2.70	119.84	2.64
1952-1961	146.84	2.59	125.94	2.56
1953-1962	148.76	2.59	125.25	2.61
1954-1963	141.36	2.58	126.30	2.48
1955-1964	135.70	2.48	127.52	2.42
1956-1965	126.16	2.49	136.80	2.47
1957-1966	125.75	2.49	134.55	2.46
1958-1967	122.62	2.45	133.00	2.38
1959-1968	115.65	2.46	136.53	2.30
1960-1969	109.42	2.36	124.75	2.37
1961-1970	115.45	2.22	128.23	2.35
1962-1971	139.15	2.10	125.21	2.38
1963-1972	160.96	2.00	136.34	2.25
1964-1973	146.05	2.15	139.62	2.28
1965-1974	145.01	2.23	146.49	2.21
1966-1975	130.28	2.27	137.79	2.19
1967-1976	136.99	2.25	137.08	2.18
1968-1977	141.34	2.29	140.50	2.16

(b)

10-year time windows in validation period	Optimized		Calculated	
	X_1(mm)	X_4(d)	X_1(mm)	X_4(d)
1978-1987	93.30	2.44	153.91	2.08
1979-1988	90.30	2.44	151.10	2.26
1980-1989	90.78	2.44	152.24	2.42
1981-1990	88.09	2.45	151.25	2.56
1982-1991	86.27	2.44	152.68	2.61
1983-1992	89.01	2.40	155.22	2.73
1984-1993	71.78	2.44	153.86	2.81
1985-1994	77.17	2.43	144.09	2.93
1986-1995	74.67	2.38	144.30	3.01
1987-1996	73.77	2.39	138.91	2.79
1988-1997	81.74	2.40	142.03	2.73
1989-1998	96.16	2.45	145.79	2.92
1990-1999	76.96	2.45	147.18	3.08
1991-2000	74.85	2.46	155.24	2.86
1992-2001	64.59	2.48	152.52	2.81

From Figure D.1 (a), for parameter X_1 (mm), the optimized values are close to calculated values with regression equation, the points are around the standard line in the calibration period. But the values show huge difference between the two sets, and the points are far from the standard line in the validation period. The values of Pearson correlation are 0.57 for calibration and 0.19 for validation. From the results, the regression equation does not show a good accuracy for estimation of parameter X_1 (mm).

In Figure D.1 (b), for parameter X_4 (d), the optimized parameter values show high similarity to the calculated values with the regression equation, and the points are around the standard line in the calibration period. But in the validation period, some of the points are close to the standard line, the others are not which show huge difference. The values of Pearson correlation are 0.83 for calibration and -0.09 for validation which means the two sets of data almost do not show any correlations.

Although the regression equations for parameter X_1 (mm) and X_4 (d) do not perform well and show a bad accuracy. However, the regression equations are the 'best' ones determined with the available data, and they are still used for simulations for GCM-RCM historical and future projections. One reason resulting in this could be from the data source, another reason could be from the optimized parameter values which are calibrated with fixed parameter X_2 (mm/d) and X_3 (mm) which can also be influence by climate change and change with a small amplitude. In this study, however, this stationary setting for parameter X_2 (mm/d) and X_3 (mm) removes the

interaction of parameters during calibration. Therefore, the optimized parameters for X_1 (mm) and X_4 (d) can be influenced.

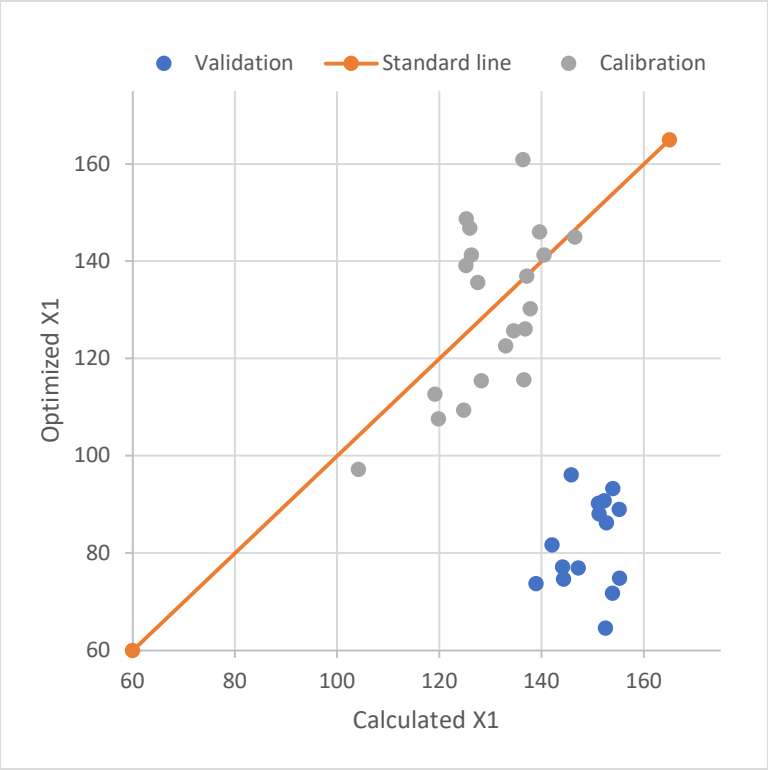

(a)

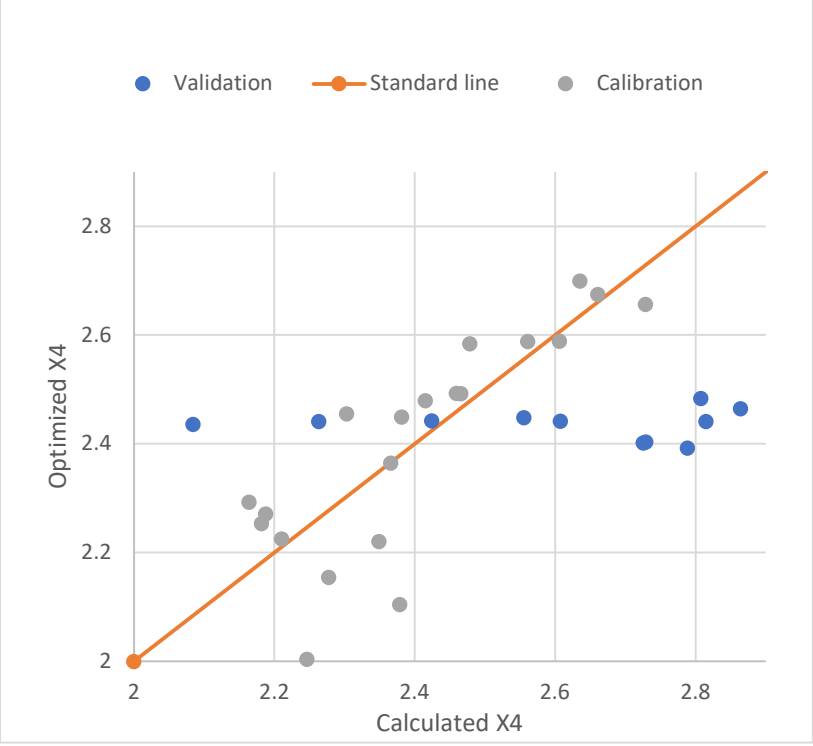

(b)

Figure D.1 Comparison of optimized and calculated parameter X_1 (mm) and X_4 (d) with the determined regression equations for the calibration period (a) and the validation period (b). The grey points mean the parameter values in the calibration period, the blue points mean the parameter values in the validation period, the red line is the standard line $y = x$.

Appendix E

Water balance analysis for each simulation period

water balance results allow an examination of the hydrological cycle for a period of time, and the purpose of the water balance is to describe the various ways in which the water supply is expended.

Table E.1 gives the annual average of precipitation (P, mm), potential evapotranspiration (PET, mm), discharge (Q, mm) and the rainfall coefficients for each case. The discharge accounts for a small part of precipitation even for the largest coefficient 0.23, which means the small bias in precipitation may lead to large discharge bias. Comparing GCM-RCM historical projection and GCM-RCM rcp4.5 or rcp8.5 projection, both annual P (mm) and annual PET (mm) increase from historical period to the first period, then to the second period. But the discharges have different changing conditions which resulted from not only P (mm) and PET (mm), but also T (°C) and model parameter sets. The comparison of the variables can also be found in Figure 4.9.

Table E.1 Values of water balance variables for observed and simulation cases.

	Water balance variables			
Cases	P(mm)	PET(mm)	Q(mm)	Q/P(-)
Observed	775.82	1382.01	115.95	0.149
Simulated-s	775.82	1382.01	108.62	0.140
Simulated-ns	775.82	1382.01	96.17	0.124
GCM-RCM hist-s	923.38	1368.97	198.20	0.215
GCM-RCM hist-ns	923.38	1368.97	171.10	0.185
Rcp4.5-2041-2070-s	847.72	1390.39	162.06	0.191
Rcp4.5-2041-2070-ns	847.72	1390.39	138.56	0.163
Rcp4.5-2071-2100-s	928.53	1400.78	193.95	0.209
Rcp4.5-2071-2100-ns	928.53	1400.78	166.33	0.179
Rcp8.5-2041-2070-s	918.18	1374.94	212.24	0.231
Rcp8.5-2041-2070-ns	918.18	1374.94	182.14	0.198
Rcp8.5-2071-2100-s	1022.96	1405.05	233.05	0.228
Rcp8.5-2071-2100-ns	1022.96	1405.05	199.21	0.195

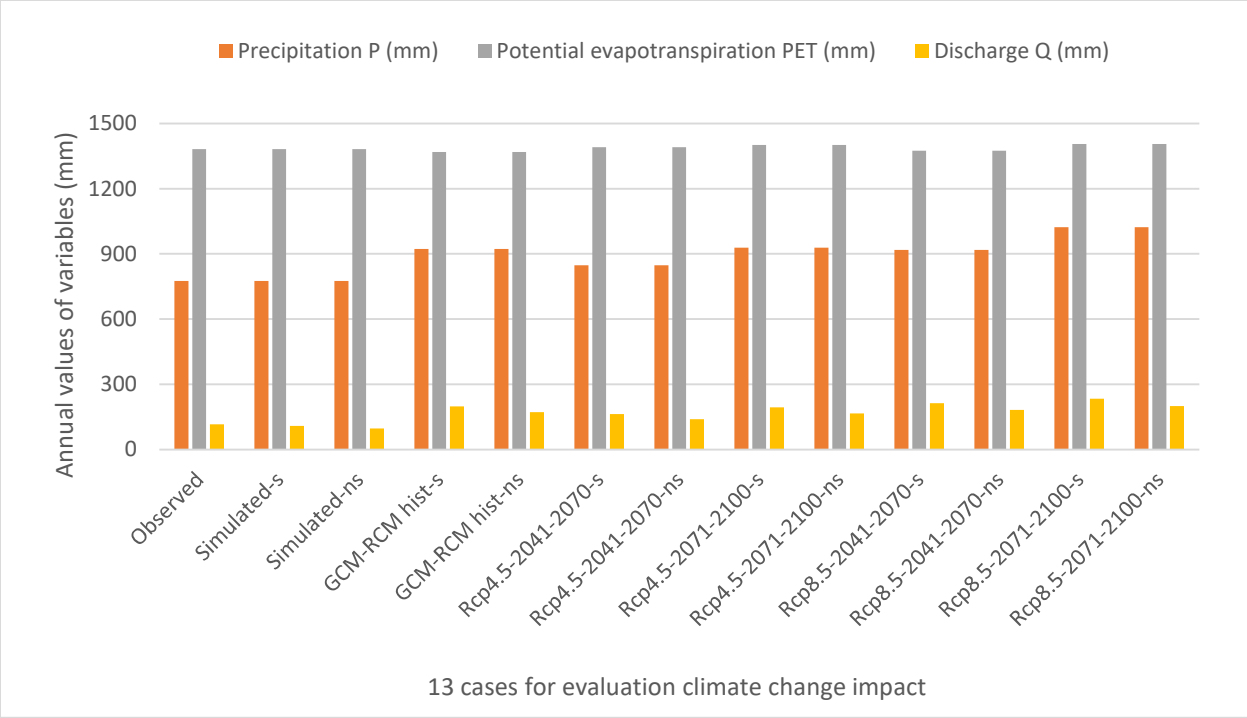

Figure E.1 Comparison between water balance variables for each case.